

Transition radiation in mechanics

A I Vesnitskiĭ, A V Metrikin

Contents

1. Introduction	983
2. Phenomenon of transition radiation in one-dimensional elastic systems	985
2.1 Transition radiation in a semibounded string. Radiation reaction and energy; 2.2 The laws of energy and momentum variation upon transition radiation of elastic waves; 2.3 Transition radiation in a semibounded beam. Loss of contact between the beam and a moving mass	
3. Transition radiation in periodically inhomogeneous one-dimensional elastic systems	990
3.1 Motion of constant load along a string resting on equispaced discrete supports. Radiation spectrum and resonance conditions; 3.2 Motion of constant load along a closed periodically inhomogeneous elastic system (spoked wheels). Resonance conditions; 3.3 Motion of mass along a string resting on a periodically inhomogeneous elastic foundation. Parametric instability of vibrations	
4. Transition radiation in randomly inhomogeneous one-dimensional elastic systems	998
4.1 Motion of constant load along a string resting on a randomly inhomogeneous elastic foundation. Limitations on the amplitude of resonance oscillations, average radiation reaction; 4.2 Motion of mass along a string resting on a randomly inhomogeneous elastic foundation. Stochastic parametric resonance	
5. Transition radiation in two-dimensional elastic systems	1002
5.1 Transition radiation in a semibounded plate. Spectral angular density of radiation energy, radiation reaction, the loss of contact between the plate and moving mass; 5.2 Motion of constant load over a membrane clamped along a half-line (diffraction radiation). Direction diagram of radiation	
6. Conclusion	1006
References	1007

Abstract. Transition radiation of elastic waves generated by a mechanical object that performs a uniform rectilinear motion along an inhomogeneous elastic system (a string, beam, membrane, or plate) is discussed in detail. The effect is analyzed by assuming that the law of motion of the load admits the generation of neither Cherenkov nor bremsstrahlung radiation and that the role of inhomogeneities is played by the supports of the elastic system. The radiation reaction spectrum and the loss of contact between the object and the elastic system are considered. The practically important cases of periodically and randomly varying elastic parameters are examined, and the resonance and instability conditions for the vibrations of the radiating object are found. Variation of the main radiation characteristics with the angle at which the object crosses the inhomogeneity region is examined. The so-called diffraction radiation of elastic waves is briefly discussed.

1. Introduction

Transition radiation is a phenomenon that arises upon a uniform rectilinear motion of a perturbation source with a

zero natural frequency in an inhomogeneous medium or near it [1]. For the first time, this phenomenon was described by V L Ginzburg and I M Frank [2] who analyzed radiation of electromagnetic waves by a charged particle crossing the boundary between an ideal conductor and vacuum. Already in early studies concerned with transition radiation, it was demonstrated that this phenomenon was universal from the physical point of view because it occurred irrespective of the physical nature of the waves. This provided a basis for the investigation into acoustic transition radiation initiated in 1962 and carried out parallel with extensive studies on electromagnetic transition radiation [3]. Today, there is a wealth of reports on both the electromagnetic and acoustic radiation, including several review papers [4, 5] and a monograph [1] published in 1984 which is in fact a comprehensive account of transition radiation in classical electrodynamics.

This review is devoted to transition radiation of elastic waves† excited by mechanical objects traveling in inhomogeneous elastic systems‡ exemplified by a railroad track. The locomotive's wheels pressed against the rails by gravity are known to excite elastic waves in the track due to track inhomogeneities caused in the main by crossties and rail joints (on Russian railroads, at least). Current collectors of a

A I Vesnitskiĭ, A V Metrikin Mechanical Engineering Institute, Russian Academy of Sciences, ul. Belinskogo 85, 603024 Nizhniĭ Novgorod, Russia
Tel. (7-831-2) 36 94 69
E-mail: a.metrikine@mav.nnov.ru

Received 6 April 1996
Uspekhi Fizicheskikh Nauk 166 (10) 1043–1068 (1996)
Translated by Yu V Morozov; edited by S N Gorin

† In this review, the term 'elastic waves' is used both in the classical sense (waves in a deformed body) and as a general name for transverse waves in a string or a membrane as well as for flexural waves in a beam or a plate resting on an elastic foundation.

‡ 'Elastic system' is a solid body, such as a string, beam, membrane, or a plate, resting on an elastic foundation and undergoing deformation.

moving electric locomotive serve as another source of elastic waves in overhead contact wires, the emission being due to clamps, fixtures, overhead switches, etc.

It would be safe to say that transition radiation of elastic waves may be observed in everyday life (suffice it to see a streetcar, trolleybus, or automobile at the entrance to a bridge). The question is how important it is to take transition radiation into consideration when analyzing the dynamics of elastic systems. It is known that the power of radiation generated by a moving source is higher the closer the source speed to the velocity of wave propagation in the medium. The average speed of modern trains in France and Japan is between 200 and 275 km h⁻¹, and the world record speed reached in France amounts to 452 km h⁻¹. The Japanese ‘500’ project to be implemented within the next decade envisions the construction of high-speed trains operated at 500 km h⁻¹. These speeds characterize elastic wave sources. As regards the wave velocities, surface waves (Rayleigh waves) are known to propagate at speeds of 400–600 km h⁻¹ in stiff roadside soils and 150–400 km h⁻¹ in soft (peat) aqueous soils. The velocities of flexural waves in the trolley wires is 200–400 km h⁻¹. It is easy to see from the comparison of these figures that the speed of an elastic wave source (train) may be equal to or even higher than the wave velocity. In some regions of Europe, where railroads lie on soft (peat) soils, surface waves produced by a running train can even be seen with the naked eye. Measurements made by railroad companies in the United Kingdom, Germany, Switzerland and France confirm increasing vibrations of the railroad track when a train moves at a speed close to surface wave velocity. This required the imposition of speed limits or strengthening ground at ‘soft’ sections of the track.

Railroad engineers make their best in attempts to reduce the ratio of the speed of trains to the speed of surface waves excited in the track without decreasing the traffic efficiency. The train speeds are chosen to be maximum possible under conditions posing no ‘elastic barrier’ problem†. In this situation, transition radiation is likely to have considerable effect on rail-track dynamics.

Let us now consider the generation of transition radiation in elastic systems. Suppose a spring-supported beam‡ resting on an elastic foundation, whose stiffness changes in the vicinity of point $x = 0$ (Fig. 1a), is subjected to a constant uniformly moving ($x = Vt$) load§ P (such a model describes an automobile driving onto a bridge or a train entering a tunnel in a rock). Far from the inhomogeneity region (Fig. 1b), the moving load carries its deformation eigenfield symmetrical with respect to the load and remaining stationary in the moving coordinate system $\xi = x - Vt$. As the load approaches the inhomogeneity region (Fig. 1c), this field undergoes a distortion; it becomes asymmetric with respect to the load and an external horizontal force $R(t)$ is needed to maintain the uniform motion of the load. Some time after the load traversed the inhomogeneity region (Fig. 1d), the

† ‘Elastic barrier’ is an analog of the sound barrier, related to the elastic wave propagation velocity.

‡ The term ‘a spring-supported beam (string, membrane, plate)’ implies that the beam (string, membrane, plate) lies on an elastic foundation. Stiffness of an elastic foundation is the summarized stiffness of the springs per unit length (for a beam and a string) or unit area (for a membrane and a plate) of the elastic system.

§ The term ‘a moving load’ is used when the elastic inertial properties of a moving mechanical object are not taken into account, and only a given vertical force is supposed to affect the elastic system at the point of contact.

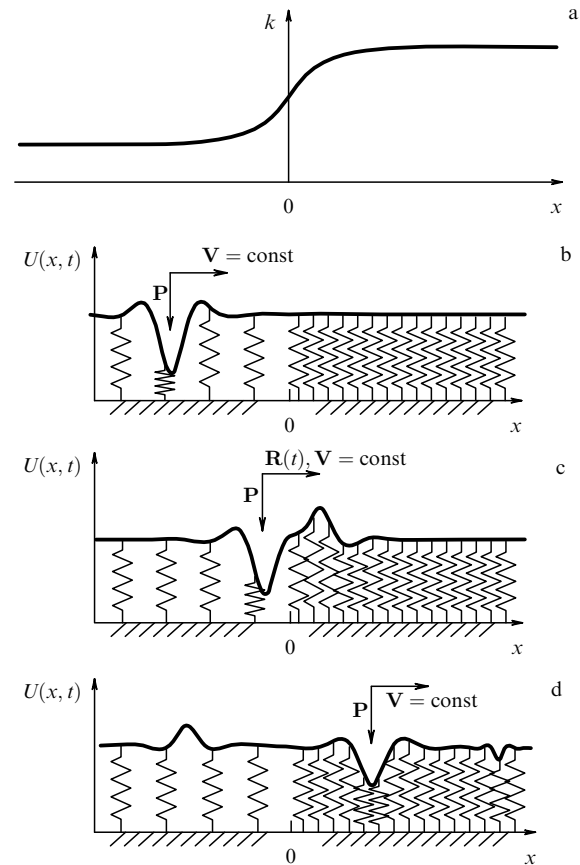


Figure 1. (a) Stiffness of the foundation. (b–d) Transformation of the deformation eigenfield of the load leading to transition radiation of elastic waves.

eigenfield becomes symmetric again. However, the eigenfield energy changes during the load transition from the ‘soft’ part of the elastic beam foundation to the ‘stiff’ one. It is this change caused by the work of forces P and $R(t)$ that gives rise to transition radiation, which actually is a portion of field energy that ‘breaks away’ in the form of free waves.

The transition radiation of elastic waves, although it is on the whole similar to that of electromagnetic and acoustic waves due to the universal physical nature of the phenomenon, displays some specific features. For instance, it may result in the loss of contact between the moving object and the elastic system. Moreover, ‘mechanical’ implications of the theory raise a number of questions that are not crucial to answer in electrodynamics and acoustics. Therefore, considerable attention has been paid in the present review both to classical problems of radiation spectrum and radiation reactions and to issues such as resonance, vibration instability, and loss of contact reported to occur during elastic wave transition radiation.

The review primarily examines one-dimensional models of elastic systems. These models are used to explicitly demonstrate physical mechanisms of the processes of interest and describe real mechanical structures. The review is organized in the following way. Section 2 analyzes ‘pure’ effects of transition radiation in cases where the law of load motion permits neither Cherenkov nor bremsstrahlung radiation of elastic waves, and the inhomogeneity is represented by the elastic-system clamping, a most typical solitary inhomogeneity in mechanics. Sections 3 and 4 deal with the practically important cases of periodic and random changes

in the elastic-system parameters. The last Section 5 explores qualitative features of transition radiation related to multi-dimensionality of elastic systems.

2. Phenomenon of transition radiation in one-dimensional elastic systems

It is appropriate to start the analysis of the phenomenon of elastic wave transition radiation from the examination of the simplest case of a mass in the field of a constant vertical force uniformly moving along a semibounded spring-supported string (Section 2.1). The role of the perturbation source in this system is played by the mass pressed against the string by force P (the analog of a charge in electrodynamics), and the inhomogeneity is represented by the point where the string is fixed (analog of the boundary with an ideal conductor). The solution to the problem will be sought in two stages. Let us first assume that the force of inertia acting vertically on the moving mass is negligible compared with the force P ; in other words, the string is affected by the constant vertical force P . In the framework of this assumption, we will try to elucidate ‘mechanical’ causes for radiation, determine the horizontal component of the reaction of the elastic system to the moving load (caused, in particular, by transition radiation), and analyze the spectral density of radiation energy. In the second stage, we intend to explore the problem as it was originally stated, that is, taking into consideration the interaction between the mass and string vibrations, which is of importance when the motion occurs at speeds close to the wave propagation velocity in the string.

As mentioned in the Introduction, transition radiation results from the transformation of the deformation eigenfield of the load during its motion in an inhomogeneous elastic system. This process is characterized in detail by the energy and momentum changes during the transition radiation of elastic waves, which will be analyzed in Section 2.2.

The string model examined in Section 2.1 fits rather well to describe vibrations in the overhead contact wire system, but it would be unwise to use it for the description of vibrations in a railroad track or a bridge. This raises the question: ‘Can qualitatively new features in elastic wave transition radiation arise from considering the flexural rigidity of an elastic system (it is the lack of flexural rigidity that is the major property distinguishing a string from a beam, which is a universally accepted model of a rail and a bridge)? We will analyze this problem in Section 2.3 concerned with the uniform motion of a mass along a semibounded hinged beam resting on an elastic foundation.

2.1 Transition radiation in a semibounded string. Radiation process, its reaction and energy

Let us consider the uniform motion ($x = Vt$) of mass m in the field of a constant vertical force P , traveling along a string that has a linear density (mass per unit length) ρ , tension N , rests on an elastic foundation with rigidity k , and is fixed at point $x = 0$ (Fig. 2). In order to analyze ‘pure’ transition radiation, let us assume that $V < c$ (c is the wave velocity in the string), i.e., no Cherenkov radiation is present.

The vertical mass and string vibrations without loss of contact are defined by the following equations [6, 7]:

$$U_{tt} - c^2 U_{xx} + h^2 U = -\frac{1}{\rho} (P + m\ddot{U}_0) \delta(x - Vt), \quad x \leq 0, \quad t \leq 0, \quad (2.1a)$$

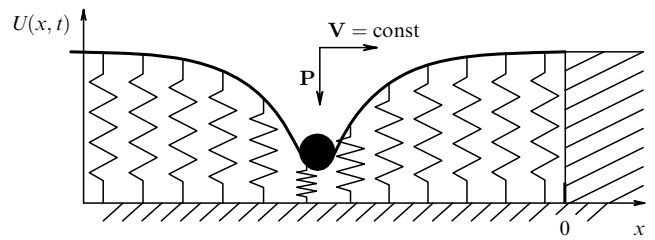


Figure 2. Uniform motion of a mass along a semibounded string.

$$U_0(t) = U(Vt, t), \quad (2.1b)$$

$$U(0, t) = 0, \quad U \rightarrow 0 \quad \text{at} \quad x - Vt \rightarrow -\infty, \quad (2.2)$$

where $c^2 = N/\rho$; $h^2 = k/\rho$; $U(x, t)$ and $U_0(t)$ are the vertical string and mass displacements, respectively; and δ is Dirac’s delta function. Equation (2.1a) represents the balance of vertical forces applied to a string element. Equation (2.1b) is in fact the condition for no loss of contact between the mass and string. The boundary conditions (2.2) indicate that the string is fixed rigidly at $x = 0$ and that its flexure tends to zero infinitely far away (to the left) from the moving mass.

Let us assume that the following condition holds at $t \leq 0$:

$$|m\ddot{U}_0| \ll P, \quad (2.3)$$

i.e., the force of inertia acting on the mass in the vertical direction is much weaker than force P . In this case, the string may be supposed to be subjected to a constant moving load P , and its vibrations can be approximately described by the equation

$$U_{tt} - c^2 U_{xx} + h^2 U = -\frac{P}{\rho} \delta(x - Vt), \quad x \leq 0, \quad t \leq 0 \quad (2.4)$$

in conjunction with the boundary conditions (2.2).

The problem (2.4), (2.2) can be solved by the method of images. Using the expression for the eigenfield of a load in a boundless spring-supported string [8]

$$U^P = -\frac{P}{2\rho h\beta} \exp\left(-\frac{h}{\beta}|x - Vt|\right), \quad \beta = \sqrt{c^2 - V^2}, \quad (2.5)$$

which satisfies Eqn (2.4) at $x \in]-\infty; \infty[$, we may represent the solution to (2.4), (2.2) as a sum of the eigenfields of the load and eigenfield of the fictitious source of force $-P$ moving in compliance with the law $x = -Vt$. In this way, we obtain the following expression for string vibrations at $t \leq 0$:

$$U^- = -\frac{P}{2\rho h\beta} \left\{ \exp\left(-\frac{h}{\beta}|x - Vt|\right) - \exp\left[\frac{h}{\beta}(x + Vt)\right] \right\}. \quad (2.6)$$

After the load passed the clamp of the string ($t \geq 0$), the string will sustain free vibrations that obey the initial conditions defined by Eqn (2.6) at $t \rightarrow 0$:

$$U^+(x, 0) = \lim_{t \rightarrow 0} U^-(x, t) = 0, \quad U_t^+(x, 0) = \lim_{t \rightarrow 0} U_t^-(x, t) = \frac{PV}{\rho\beta^2} \exp\frac{hx}{\beta}. \quad (2.7)$$

The initial conditions (2.7) imply that the string energy is non-zero as the load passes the clamp ($t = 0$), and it is this circumstance that accounts for string oscillations at $t > 0$.

According to [8], string displacements at $t > 0$ are defined by the expression

$$U^+(x, t) = \frac{P}{\rho h \beta} \left\{ \sinh \frac{hVt}{\beta} \exp \frac{hx}{\beta} - \sinh \left[\frac{h}{\beta} (x + Vt) \right] \Theta(x + ct) \right\} + \frac{PV}{\pi \rho} \Theta(x + ct) \int_{-h}^h \frac{\sinh(x\sqrt{h^2 - z^2}/c) \cos tz}{z^2(c^2 - V^2) + h^2V^2} dz.$$

Figure 3 shows string profiles at different time moments. At the beginning, the load carries its eigenfield. As the load approaches the clamp, the field undergoes a distortion (due to image effects) and becomes asymmetric with respect to the load. When the load crosses the clamp, the string has zero potential energy and nonzero kinetic energy. At $t > 0$, the profile shows a pulse running to the left of the clamp (with a bend at the top) traveling at speed c . It is precisely this pulse (whose shape varies in time due to wave dispersion in the spring-supported string and due to string-clamp interaction that represents the transition radiation of elastic waves.

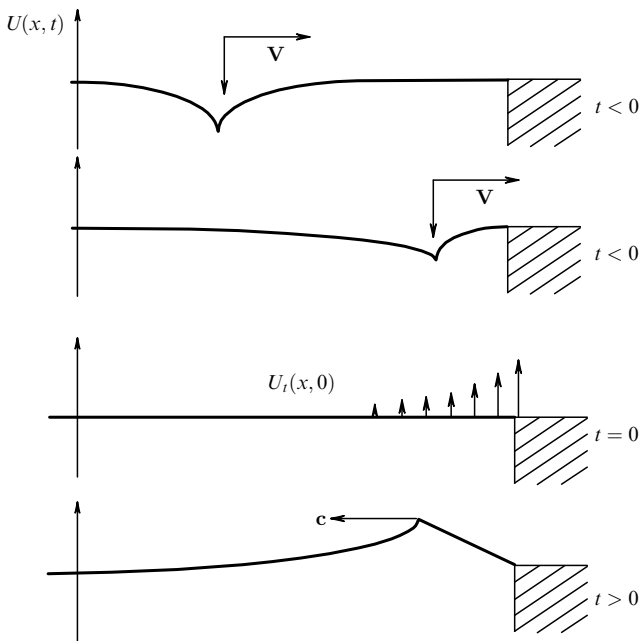


Figure 3. Profiles of a string subjected to a moving load as it traverses the clamp and after this (when the string undergoes free vibrations).

Now, let us find radiation energy W^r . Disregarding viscous losses, the energy stored in the string at $t = 0$ is equal to the radiation energy, i.e., $W^r = H(0)$, where

$$H(t) = \frac{1}{2} \int_{-\infty}^0 (\rho U_t^2 + N U_x^2 + k U^2) dx$$

is the energy of a semiinfinite string ($x \leq 0$) resting on an elastic foundation. Substitution of (2.7) yields

$$W^r = \frac{1}{2} \int_{-\infty}^0 \rho U_t^2(x, 0) dx = \frac{P^2 V^2}{4 \rho h \beta^3}. \tag{2.8}$$

It appears from (2.8) that the transition radiation energy increases as the speed of the load approaches the wave velocity in the string. Evidently, the radiation reaction must equally grow, leading to the rapid wear of the elastic construction. Since radiation propagates along the string, the reaction must also act in a horizontal direction. According to [6], the expression for the horizontal component of the string reaction has the form

$$F^r = -\frac{P}{2} (U_x(Vt + 0, t) + U_x(Vt - 0, t)).$$

Substitution of (2.6) into this expression results in

$$F^r = -\frac{P^2}{2 \rho \beta^2} \exp \frac{2hVt}{\beta}. \tag{2.9}$$

Therefore, the horizontal reaction of the string actually grows with increasing load speed. Moreover, it increases as the load approaches the clamp. In the railroad overhead contact wire system, structures holding the current-carrying wire are the ‘weakest link’ of the system. It cannot be otherwise, as follows from Eqn (2.9), because mechanical stresses in the wire increase dramatically as the current collector traverses the clamps. Both the transition radiation reaction and the reaction of the deformation field arising near the clamps are responsible for the enhanced stress.

The work done by the horizontal component of the string reaction is described by the expression

$$W^f = V \int_{-\infty}^0 F^r dt = -\frac{P^2}{4 \rho h \beta}. \tag{2.10}$$

Note that the radiation energy increases in proportion to V^2/β^3 as the motion becomes faster, whereas the work of the horizontal reaction of the string grows as $1/\beta$. This difference in the laws of energy growth indicates once again that the work necessary to slow down a load is done by both the deformation field of radiation formed and the deformation field localized near the clamp.

Let us now find the spectral density of radiation energy. This radiation parameter can be quantified with up-to-date measuring instruments and used to evaluate the state of elastic systems interacting with moving objects.

Applying the integral Fourier transformation with respect to time

$$V_\omega(x, \omega) = \int_{-\infty}^{\infty} U(x, t) \exp i\omega t dt. \tag{2.11}$$

to (2.4), (2.2) yields

$$c^2 \frac{\partial^2}{\partial x^2} V_\omega + (\omega^2 - h^2) V_\omega = \frac{P}{\rho \omega} \exp \frac{i\omega x}{V}, \tag{2.12}$$

$$V_\omega(0, \omega) = 0. \tag{2.13}$$

The solution to (2.12), (2.13) with regard for the conditions at infinity (string displacement tending to zero at $|\omega| < h$ and energy removed from the clamp at $|\omega| > h$) has the form

$$V_\omega = V_\omega^p + V_\omega^r = -a(\omega) \left[\exp \frac{i\omega x}{V} - \exp \left(-\frac{ix\sqrt{\omega^2 - h^2}}{c} \right) \right], \tag{2.14}$$

The first term in (2.14) describes the eigenfield of the load, while the second one characterizes free waves that represent transition radiation at $|\omega| > h$.

The radiation energy is equal to the energy flux through the cross section $x \rightarrow -\infty$ taken with the inverse sign and integrated with respect to time (see [8]):

$$W^r = N \int_{-\infty}^{\infty} U_x U_t \Big|_{x \rightarrow -\infty} dt = -\frac{N}{4\pi^2 c} \iiint_{-\infty}^{\infty} \omega \sqrt{\omega_1^2 - h^2} \times a(\omega) a(\omega_1) \exp[-it(\omega + \omega_1)] \times \exp\left[-ix\left(\sqrt{\omega^2 - h^2} + \sqrt{\omega_1^2 - h^2}\right)\right] \Big|_{x \rightarrow -\infty} d\omega d\omega_1 dt.$$

Integration with respect to time yields a delta function, which allows the integral to be taken for ω_1 to obtain

$$W^r = \frac{N}{\pi c} \int_h^{\infty} \omega \sqrt{\omega^2 - h^2} a^2(\omega) d\omega. \tag{2.15}$$

The spectral density of radiation

$$S(\omega) = \frac{N}{\pi c} \omega \sqrt{\omega^2 - h^2} a^2(\omega)$$

for various load speeds V is shown in Fig. 4. $S(\omega)$ is seen to have a maximum that is shifted to the high-frequency region with increasing V . At $\omega \rightarrow \infty$, the spectral density of the radiation energy decreases as $1/\omega$. Note that taking integral in (2.15) yields (2.8).

We have so far neglected mass inertia (see the condition (2.3)). Let us now check whether the solution to (2.6) satisfies condition (2.3). Comparison of the two expressions reveals that inertia of the mass may be neglected provided the inequality

$$\frac{V^2}{(c^2 - V^2)^{3/2}} \ll \frac{2\rho}{hm} \tag{2.16}$$

is fulfilled. It is clear that condition (2.16) is not satisfied at $V \rightarrow c$ and $m/\rho \rightarrow \infty$. Hence, for fast-speed heavy objects inertia cannot be disregarded.

Let us analyze the initial problem (2.1), (2.2). Using the method of images, it can be rewritten as

$$U_{tt} - c^2 U_{xx} + h^2 U = -\frac{1}{\rho} (P + m\ddot{U}_0) \times [\delta(x - Vt) - \delta(x + Vt)], \quad x \leq 0, \quad t \leq 0, \\ U_0(t) = U(Vt, t). \tag{2.17}$$

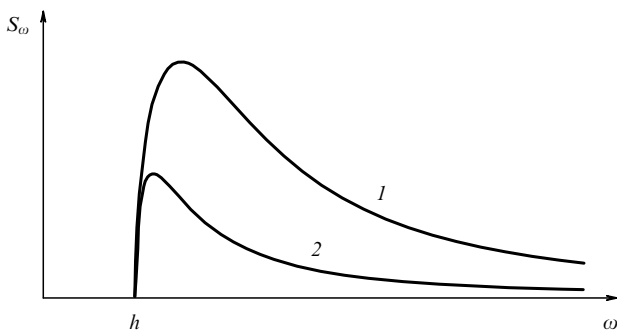


Figure 4. Spectral density of transition radiation energy at different load speeds: (1) $V = 0.8c$; (2) $V = 0.4c$.

Because of the problem's linearity, the solution to (2.17) must be sought in the form

$$U = U^- + U^m,$$

where U^- is the solution to (2.4) described by expression (2.6) and U^m is the solution to

$$U_{tt} - c^2 U_{xx} + h^2 U = -\frac{m}{\rho} \ddot{U}_0 [\delta(x - Vt) - \delta(x + Vt)]. \tag{2.18}$$

Using (2.6) and the fundamental solution for the operator

$$\frac{\partial^2}{\partial t^2} - c^2 \frac{\partial^2}{\partial x^2} + h^2$$

of the form

$$\frac{J_0[(h/c)\sqrt{c^2 t^2 - x^2}] \Theta(ct - |x|)}{2c}$$

(where J_0 is the zero-order Bessel function and Θ is the unit function), the expression for $U(x, t)$ may be written as

$$U = -\frac{P}{2\rho h\beta} \left[\exp\left(-\frac{h|x - Vt|}{\beta}\right) - \exp\frac{h(x + Vt)}{\beta} \right] + \frac{m}{2\rho c} \times \begin{cases} \int_{-\infty}^{\mu^+/\Delta^-} \ddot{U}_0(\tau) J_0(v^+) d\tau - \int_{-\infty}^{\mu^+/\Delta^+} \ddot{U}_0(\tau) J_0(v^-) d\tau, & x \leq Vt, \\ \int_{-\infty}^{\mu^+/\Delta^+} \ddot{U}_0(\tau) J_0(v^+) d\tau - \int_{-\infty}^{-\mu^-/\Delta^-} \ddot{U}_0(\tau) J_0(v^-) d\tau, & x \geq Vt, \end{cases} \tag{2.19}$$

where $\mu^\pm = x \pm ct$, $\Delta^\pm = c \pm V$,

$$v^\pm(x, t, \tau) = \frac{h}{c} \sqrt{c^2(t - \tau)^2 - (x \pm Vt)^2}.$$

The unknown $U_0(t)$ can be found using the continuity condition for no loss of contact between the string and mass, $U_0(t) = U(Vt, t)$. For $x = Vt$, we obtain

$$U_0(t) = -\frac{P}{2\rho h\beta} \left(1 - \exp\frac{2hVt}{\beta} \right) + \frac{m}{2\rho c} \left[\int_{-\infty}^{t\Delta^+/\Delta^-} \ddot{U}_0(\tau) J_0(v^+(Vt, t, \tau)) d\tau - \int_{-\infty}^t \ddot{U}_0(\tau) J_0(v^-(Vt, t, \tau)) d\tau \right]. \tag{2.20}$$

The integro-differential Eqn (2.20) is reduced by term-by-term differentiation to the Volterra integral equation of the second kind in $\ddot{U}_0(t)$, which is convenient to use in numerical analysis. Figure 5 qualitatively depicts $\ddot{U}_0(t)$ dependences for different V . It is clear that the load $P + m\ddot{U}_0(t)$ vertically applied to the string increases as the mass approaches the clamp. Naturally, this must lead to a rise in both the radiation energy and radiation reaction (this self-evident fact is confirmed by calculations). Therefore, taking into consideration mass inertia in the framework of the 'string' model results in increased transition radiation power.

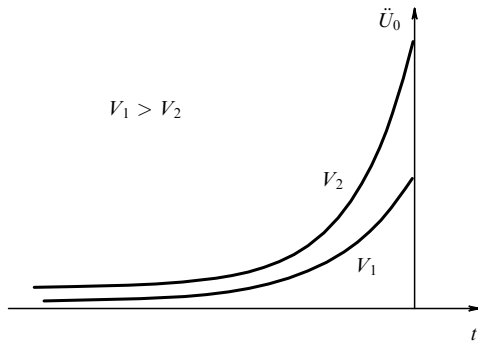


Figure 5. Time dependence of the vertical acceleration of the mass at different load speeds.

2.2 The laws of energy and momentum variation upon transition radiation of elastic waves

Transition radiation originates from changes in the deformation eigenfield of a perturbation source in an inhomogeneous medium. What forces are responsible for the work needed to maintain this process? What momentum is transferred to the elastic system? Analysis of the laws of energy and momentum variation below may help to answer these questions and better understand physical mechanisms underlying transition radiation. For simplicity, let us use the case of a string subjected to a moving load as described in Section 2.1.

2.2.1 The law of the energy variation. Let us first determine the energy of the deformation eigenfield W^P . Using (2.5) and the general expression for the energy of a spring-supported string (see Ref. [6]), we obtain

$$W^P = \frac{1}{2} \int_{-\infty}^{\infty} \left[\rho V^2 (U_{\xi}^P)^2 + N (U_{\xi}^P)^2 + k (U^P)^2 \right] d\xi = \frac{P^2 c^2}{4\rho h \beta^3}. \tag{2.21}$$

When the load crosses the clamp, the energy of the deformation eigenfield is zero, that is, its change ΔW^P is $-W^P$.

As noted in Section 2.1, in the vicinity of the clamp the load is subjected to a horizontal force of the resistance to motion F^r . Hence, a uniform motion of the load along the string can be maintained if an external force R , which is equal to F^r in magnitude but has the opposite direction, is applied to the load. The work done by force R is determined by the opposite-signed expression (2.10).

It is obvious that the point of contact between the load and the string near the clamp moves not horizontally. Therefore, work is also done by the vertical force P . The work A^P of this force is defined by the equation

$$A^P = -P \left[U^-(0, 0) - \lim_{t \rightarrow -\infty} U^-(Vt, t) \right] = -\frac{P^2}{2\rho h \beta}. \tag{2.22}$$

Comparing (2.21), (2.22), and (2.10) with the expression for the radiation energy (2.8), we may write the law of energy variation as

$$W^r = -\Delta W^P + W^R + A^P. \tag{2.23}$$

Thus, it follows from (2.23) that the motion of the load is associated with the transformation of the eigenfield energy to the radiation energy, with work being done by both the external force R , which maintains the uniform movement of

the load, and the vertical force P (the load itself). Note that all the quantities in Eqn (2.23) are bounded, unlike those in the expressions for energy variation in electrodynamics [1]. This can be accounted for by the absence of a jump in dimensionality between a zero-dimensional (pointlike) perturbation source and a one-dimensional waveguide (in electrodynamics, the zero-dimensional charge perturbs the three-dimensional medium).

The question that now arises is whether the law of energy variation is violated when mass inertia cannot be neglected [condition (2.3) is not fulfilled]. The answer is ‘yes’ because the velocity of mass crossing the clamp has a vertical component V_U , and a term $-mV_U^2/2$ appears in the right-hand side of Eqn (2.23). In the general case, if the moving object has internal degrees of freedom (e.g., two-mass oscillator), the law of energy variation for transition radiation has the form

$$W^r = -\Delta W^P + W^R + A^P - \left(E - \frac{MV^2}{2} \right),$$

where E is the mechanical energy of the object when it passes the clamp and M is its total mass. If the object’s inertia (in the general case, internal degrees of freedom) is taken into account, the expressions for ΔW^P and A^P remain unaltered, whereas W^R and W^r change.

2.2.2 The law of momentum variation. The deformation eigenfield, which moves together with the load, transfers not only energy, but also momentum (note that, the problem of wave momentum in elastic systems remains a matter of controversy [9]). Using the general expression for the wave momentum in a string and Eqns (2.5), we obtain the equation for the momentum of the eigenfield p^P

$$p^P = -\rho \int_{-\infty}^{\infty} U_x^P U_t^P dx = \frac{P^2 V}{4\rho h \beta^3}. \tag{2.24}$$

Note the simple relation between the energy and the momentum of the eigenfield: $W^P = (c^2/V)p^P$, which reduces to $W^P = cp^P$ at $V \rightarrow c$.

During the eigenfield transformation, an additional momentum is introduced into the elastic system, which is due to the action of force R that maintains the uniform motion of the load. The momentum p^R due to this force is defined by the expression [see (2.9)]

$$p^R = \int_{-\infty}^0 R dt = - \int_{-\infty}^0 F^r dt = \frac{P^2}{4\rho h \beta V}. \tag{2.25}$$

The string does not only receive momentum from force R , but also transfers momentum p^T to the clamp. As inferred from the general expression for the horizontal force T that acts on an obstacle from the spring-supported string [6], the following momentum is transferred to the clamp at $t \leq 0$ (i.e., while the load moves along the string):

$$p_{t=0}^T = \int_{-\infty}^0 T(0, t) dt = \frac{P^2 c^2}{4\rho h V \beta^3}, \tag{2.26}$$

where

$$T(x, t) = \frac{1}{2} \left[\rho (U_t^-)^2 + N (U_x^-)^2 - k (U^-)^2 \right].$$

Since no string displacement occurred when the load crossed the clamp ($t = 0$), its horizontal (wave-related)

momentum was zero, and the entire momentum of the system was stored in the clamp. Indeed, it appears from a comparison of (2.24), (2.25), and (2.26) that the law of momentum variation at $t \leq 0$ has the form

$$p^P + p^R = p_{t=0}^T. \tag{2.27}$$

At $t \geq 0$, the ‘exchange’ of momenta between the string and the clamp continues, and part of the momentum is carried away with radiation onto infinity. Therefore, the law of momentum variation has now the form

$$p^r = p_{t=0}^T - p^T, \tag{2.28}$$

where p^r is the momentum of transition radiation and p^T is the total momentum transferred to the clamp for time $t \in]-\infty; \infty[$. The radiation momentum is determined by the expression

$$p^r = -\frac{P^2}{2\pi\rho hV\beta^3} \left[\beta V + (2V^2 - c^2) \left(\frac{\pi}{2} - \arctan \frac{\beta}{V} \right) \right]. \tag{2.29}$$

Note that p^r is a negative quantity, which is natural since the radiation propagates to the left. Expression (2.29) was obtained using the solution to the problem in the spectral form (2.14) by the method described in Ref. [1]. The momentum p^T is actually the difference between (2.26) and (2.29).

By eliminating $p_{t=0}^T$ from (2.27) and (2.28), we can write the integral law of momentum variation during transition radiation (the form of the law remains unaltered even if inertia of a moving object is taken into account):

$$p^r = p^P + p^R - p^T. \tag{2.30}$$

Thus, in transition radiation of elastic waves, the momentum of the load’s eigenfield is transferred to both the radiation and the clamp (or to the inhomogeneity region, in the general case of an arbitrarily inhomogeneous elastic system). Concurrently, an additional momentum is introduced into the elastic system due to the force R which maintains the uniform motion of the load.

The process of momentum transfer described by (2.30) is similar to the process that occurs when an elastic ball strikes a wall. Indeed, the integrated law of momentum variation for such a collision may be written as (2.30) on the assumption that a force R presses the ball against the wall for some time during the contact between them. In this case, the terms in (2.30) describe the following quantities: $p^P = mV$ is the momentum of the ball before it strikes the wall, p^R is the momentum introduced into the ball–wall system by force R , $p^T = 2mV + x$ is the momentum transferred to the wall during the contact, $p^r = -mV + y$ is the momentum of the reflected ball ($x + y = p^R$). Such an analogy appears natural in the context of the wave-corpucle duality principle and allows the process of radiation to be represented as the fall of a quasiparticle (deformation eigenfield) onto a clamp followed by its bouncing (reflection). It is the reflected portion of the energy–momentum that represents transition radiation.

2.3 Transition radiation in a semibounded beam.

Loss of contact between the beam and a moving mass

The elastic system model (a spring-supported string) described in Section 2.1 provided a valuable tool for a detailed

qualitative examination of specific features of transition radiation in one-dimensional elastic systems. However, this model does not take into account flexural rigidity which is intrinsic, to a certain extent, in all elastic guides. Hence, the problem of flexural rigidity effect on the radiation process arises.

To solve this problem, let us consider the motion of a mass along a semibounded spring-supported beam (Fig. 6). In terms of the wave–particle duality concept, flexural rigidity does not interfere in this situation. Similar to the case of mass moving along a string, a deformation eigenfield travels together with the mass along such a beam and must be reflected from the clamp, converting into transition radiation. However, this transition radiation arises through a mechanism that is qualitatively different from that underlying the mass–string interaction. The difference is due to the fact that the deformation eigenfield in a beam falls off nonmonotonically with the distance from the moving mass, in agreement with the expression describing this field [10] (see also Fig. 7):

$$U^P = -A \exp(-s_1|\xi|) \left(\cos s_2\xi + \frac{s_1}{s_2} \sin s_2|\xi| \right), \tag{2.31}$$

where $A = P/(8EI s_1 \mu^2)$; $s_1 = \sqrt{\mu^2 - V^2 v^2}$; $s_2 = \sqrt{\mu^2 + V^2 v^2}$; $\xi = x - Vt$; $4\mu^4 = k/EI$; $4v^2 = \rho/EI$; EI and ρ are the flexural rigidity and the linear density of the beam, respectively; k is the stiffness of the elastic base; and V is the mass velocity. This non-monotonical process is responsible for vertical vibrations of the mass as it moves near the clamp, which may cause the loss of mass–beam contact. Such loss of contact is likely to occur also when a mass moves along a string, but only as it crosses the clamp.

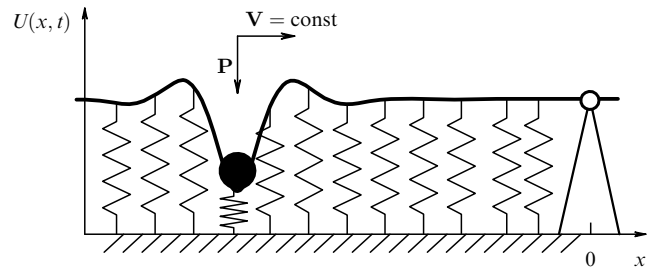


Figure 6. Uniform motion of a mass along a hinged semibounded beam.

No-loss-of-contact vibrations of a uniformly ($x = Vt$) moving mass m pressed by a vertical force P against an Euler–Bernoulli beam [11] fixed by a hinge at $x = 0$ are described by the following system of equations [7]:

$$\begin{aligned} U_{xxxx} + 4v^2 U_{tt} + 4\mu^4 U &= -\frac{1}{EI} (P + m\ddot{U}_0) \delta(x - Vt), \\ x \leq 0, \quad t \leq 0, \\ U(Vt, t) &= U_0(t), \quad U(0, t) = U_{xx}(0, t) = 0, \\ U \rightarrow 0 \quad \text{at} \quad x - Vt &\rightarrow -\infty, \end{aligned} \tag{2.32}$$

where $U(x, t)$, $U_0(t)$ are the vertical displacements of the beam and the mass, respectively.

The solution to the problem (2.32) at $V < V_{cr} = \mu/v$ (V_{cr} is the minimal phase velocity of flexural waves in the beam) can be obtained by the method of images. Because the

problem of a moving load ($m\ddot{U}_0 \ll P$) has in this case no qualitatively new features, the solution may straightforwardly be written with the allowance for mass inertia:

$$U(x, t) = -A \exp(-s_1|\xi|) \left(\cos s_2\xi + \frac{s_1}{s_2} \sin s_2|\xi| \right) + A \exp s_1\eta \left(\cos s_2\eta - \frac{s_1}{s_2} \sin s_2\eta \right) + \frac{m}{2\rho} \int_{-\infty}^t \ddot{U}_0(\tau) R(x, t, \tau) d\tau, \quad x \leq 0, \quad t \leq 0,$$

where $\xi = x - Vt$, $\eta = x + Vt$, $\lambda = \sqrt{k^4 + 4\mu^4}/2v$, A is defined in (2.31), and

$$R(x, t, \tau) = \int_0^\infty \frac{1}{\lambda} \sin[\lambda(t - \tau)] \times \left\{ \cos[k(x + V\tau)] - \cos[k(x - V\tau)] \right\} dk.$$

By using the condition of continuous contact $U(Vt, t) = U_0(t)$, we obtain the following integro-differential equation for the vertical mass displacement:

$$U_0(t) = \frac{m}{2\rho} \int_{-\infty}^t \ddot{U}_0(\tau) R(Vt, t, \tau) d\tau - A + A \exp(2s_1 Vt) \left(\cos 2s_2 Vt - \frac{s_1}{s_2} \sin 2s_2 Vt \right). \quad (2.33)$$

The result of numerical analysis of (2.33) is presented in Fig. 7 in the form of the $\ddot{U}_0(t)$ dependence. It can be seen that vertical mass oscillations occur near the clamp. Also, it is evident that the condition $\ddot{U}_0(t^*) = -P/m$ can be fulfilled at a time moment $t^* < 0$, which means that the beam reaction for the moving mass vanishes, i.e., the mass–beam contact is lost (the system of equations (2.32) and Eqn (2.33) are valid only at $t < t^*$). Fig. 8 shows the curve separating the qualitatively different modes of the system’s behavior on the plane of parameters $M = m\mu/\rho$ (dimensionless mass) and $\alpha = V/V_{cr}$ (dimensionless velocity). The area above the curve corresponds to the motion with loss of contact at $t < 0$.

Thus, upon the motion of an object along a nonuniform elastic guide, loss of contact between the object and the guide

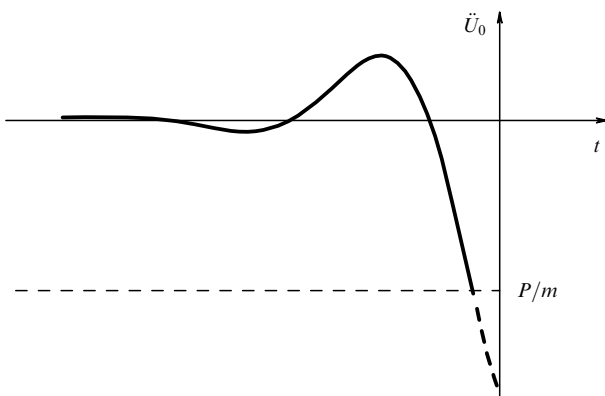


Figure 7. Time dependence of vertical mass acceleration. Note the loss of mass–beam contact at $\ddot{U} = -P/m$.

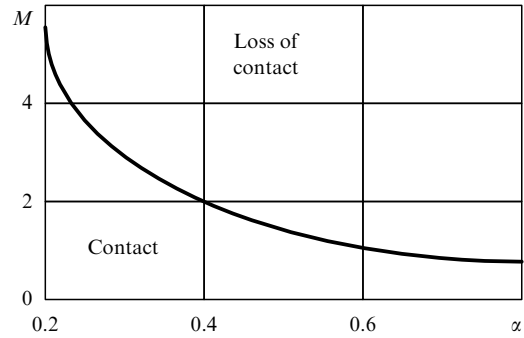


Figure 8. The curve dividing the plane of parameters (α, M) into contact and noncontact regions of mass and beam motion.

can occur during transition radiation. This feature of transition radiation in elastic systems has a very important practical implication, since it is the loss of the object–guide contact that is responsible for sparking in a current-collecting system or a sharp rise in the level of vibrations of railroad trains.

3. Transition radiation in periodically inhomogeneous one-dimensional elastic systems

A train catenary, a railroad track, and a guideway for a magnetically levitated vehicles [12] may all be regarded as periodically inhomogeneous elastic systems due to the effects of contact – line supports, crossties, and piers, respectively. Investigations into the dynamics of periodically inhomogeneous elastic systems are, therefore, of crucial importance in practical application [13]. Main research trends are also dictated by practical considerations and include elucidation of the mechanisms which underlie resonance effects and the problem of instability of vibrations in a moving object–elastic guide system. Transition radiation is the primary cause of these undesirable phenomena. Specifically, resonance is due to the discreteness of the radiation spectra in periodic systems and occurs when the group velocity of an emitted harmonic coincides with the load speed. The instability of vibrations results from the reaction for the radiation of anomalous Doppler waves [14–17].

This section is concerned with three problems. First, we will discuss the motion of a load along a periodically inhomogeneous boundless elastic system and use the solution of this problem to analyze the spectrum, the radiation reaction averaged over the inhomogeneity period, and the conditions for the development of resonance in an elastic system [12, 18–20]. Second, we will briefly consider the motion of a load in a closed periodically inhomogeneous elastic system (spoked wheel) [21]. The latter problem is of special interest in the context of the noise abatement program for the EEC railroad network, which envisions a new wheel design for cars in the form of a steel spoked wheel rim (as opposed to the currently used all-metal wheels). It appears appropriate to discuss load-induced wheel vibrations in this section because they result from transition radiation, with special reference to resonance conditions. Third, we will consider the problem of coupled vibrations of a moving object and a periodically inhomogeneous guide [22]. It will be demonstrated that the allowance for coupling leads to the appearance of zones of vibration instability in an object–guide system.

3.1 Motion of constant load along a string resting on equispaced discrete supports. Radiation spectrum and resonance conditions

Let us consider the uniform motion ($x = Vt$) of a constant vertical load P along a boundless string lying on equally spaced discrete elastic inertial supports (Fig. 9). This model satisfactorily describes vibrations of the current wire excited by the current collector of a moving locomotive; also, it is simple to analyze. Steady state oscillations of the string are described in the linear approximation by the following system of equations:

$$\begin{aligned}
 U_{tt} - c^2 U_{xx} &= -\frac{P}{\rho} \delta(x - Vt), & c^2 &= \sqrt{\frac{N}{\rho}}, \\
 -\infty < x < \infty, & & -\infty < t < \infty, \\
 U(nd, t) &= U_n^0(t), \\
 N[U_x(nd + 0, t) - U_x(nd - 0, t)] &= m\ddot{U}_n^0 + \delta\dot{U}_n^0 + kU_n^0,
 \end{aligned}
 \tag{3.1}$$

where $U(x, t)$ is the transverse displacement of the string; U_n^0 is the vertical displacement of mass of the n th support; N and ρ are the tension and the linear density of the string, respectively (henceforth, we will assume $V < c = \sqrt{N/\rho}$); d is the distance between the neighboring supports; $m, k,$ and δ are the mass, rigidity, and viscosity of a support respectively; and $n = 0, \pm 1, \pm 2, \dots$

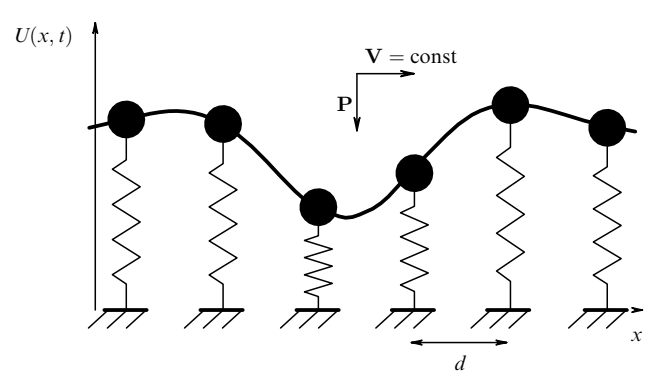


Figure 9. The motion of a constant load along a string resting on equally spaced supports.

By applying to (3.1) the integral Fourier transformation (2.11) with respect to time, we obtain

$$\begin{aligned}
 \frac{\partial^2}{\partial x^2} V_\omega + \frac{\omega^2}{c^2} V_\omega &= \frac{F}{V} \exp \frac{i\omega x}{V}, \\
 V_\omega(nd, \omega) &= V_{\omega n}^0(\omega), \\
 N \frac{\partial}{\partial x} [V_\omega(nd + 0, \omega) - V_\omega(nd - 0, \omega)] \\
 &= (k - i\delta\omega - m\omega^2) V_{\omega n}^0(\omega),
 \end{aligned}
 \tag{3.2}$$

where $V_{\omega n}^0(\omega)$ are the Fourier transforms of the displacement of the n th mass, and $F = P/\rho c^2$.

The system (3.2) can be solved using the periodicity condition [20] related to the system's periodicity and the

uniformity of the load motion. The solution to the initial system (3.1) has the form

$$U(x, t) = U\left(x + nd, t + \frac{nd}{V}\right)
 \tag{3.3}$$

and means that the string in the steady-state regime periodically ($T = d/V$) reproduces its own shape although with a spatial shift equal to the structure period d . In the transform space, the condition (3.3) has the form

$$V_\omega(x + nd, \omega) = V_\omega(x, \omega) \exp \frac{i\omega nd}{V}.
 \tag{3.4}$$

Writing the general solution (3.2) for $x \in [0, d]$

$$\begin{aligned}
 V_\omega &= A \exp \frac{i\omega x}{c} + B \exp\left(-\frac{i\omega x}{c}\right) - S \exp \frac{i\omega x}{V}, \\
 S &= \frac{FVc^2(c^2 - V^2)}{\omega^2}
 \end{aligned}
 \tag{3.5}$$

and using the periodicity condition (3.4), we obtain the following expressions for V_ω and $V_{\omega n}^0$ at arbitrary x and n :

$$\begin{aligned}
 V_\omega &= \exp \frac{i\omega nd}{V} \left[A \exp \frac{i\omega(x - nd)}{c} + \right. \\
 &\quad \left. + B \exp\left(-\frac{i\omega(x - nd)}{c}\right) \right] - S \exp \frac{i\omega x}{V}, \\
 V_{\omega n}^0 &= C \exp \frac{i\omega nd}{V}.
 \end{aligned}$$

The joining of the solutions at $x = 0$ and $x = d$ yields a system of linear equations with respect to $A, B,$ and $C,$ whose solution results in

$$\begin{aligned}
 A &= \frac{\Delta_A}{\Delta}, & B &= \frac{\Delta_B}{\Delta}, & C &= \frac{\Delta_C}{\Delta}, \\
 \Delta &= -2\beta[p^2 + 1 - p(\gamma^- + \gamma^+) - Gp(\gamma^- + \gamma^+)] \\
 &= -4\beta p \left(\cos \frac{\omega d}{V} - \cos \frac{\omega d}{c} - \frac{Gc}{2\omega} \sin \frac{\omega d}{c} \right), \\
 \Delta_1 &= SGp(p - \gamma^-), & \Delta_2 &= SGp(\gamma^+ - p), \\
 \Delta_3 &= 2\beta S[p^2 + 1 - p(\gamma^- + \gamma^+)], \\
 \beta &= \frac{i\omega}{c}, & \gamma^\pm &= \exp\left(\pm \frac{i\omega d}{c}\right), & p &= \exp \frac{i\omega d}{V}, \\
 G &= \frac{k - m\omega^2 - i\delta\omega}{N}.
 \end{aligned}$$

The application of the inverse Fourier transformation to (3.5) brings about the exact solution at $x \in [0, d]$:

$$\begin{aligned}
 U(x, t) &= \frac{1}{2\pi} \int_{-\infty}^{\infty} \frac{S}{\Delta} \left\{ Gp \left[(p - \gamma^-) \exp \frac{i\omega x}{c} \right. \right. \\
 &\quad \left. \left. + (\gamma^+ - p) \exp\left(-\frac{i\omega x}{c}\right) \right] - \Delta \exp \frac{i\omega x}{V} \right\} \exp(-i\omega t) d\omega.
 \end{aligned}
 \tag{3.6}$$

The string displacements at $x \notin [0, d]$ are estimated from the periodicity condition (3.3).

The poles of the integrand in (3.6) that determine the frequencies of harmonics produced by the load are roots of the equation

$$\cos[\tilde{k}(\omega)d] = \cos \frac{\omega d}{V}, \tag{3.7}$$

where

$$\cos[\tilde{k}(\omega)d] = \cos \frac{\omega d}{c} + \frac{Gc}{2\omega} \sin \frac{\omega d}{c}$$

is the dispersion equation for a string resting on equispaced inertial viscoelastic supports. Figure 10 illustrates the graphical solution of Eqn (3.7) at $\delta \rightarrow 0$ from which the real roots of this equation can be inferred. Evidently, the radiation spectrum is discrete. The frequencies of the emitted harmonics are defined by intersections of the discontinuous curve (dispersion dependence of the periodically inhomogeneous system) and a family of monotonically sloping curves (kinematic invariants ‘monitoring’ phase equality of the emitted harmonics and the load in the contact point). The discrete spectrum of the radiation is created in the following way. As the load crosses a support, transition radiation with a continuous spectrum is formed. The radiation fields excited by the load on its passage across each support are phased at certain frequencies due to the elastic-system is periodicity. This accounts for the discrete radiation spectrum in the steady-state regime with harmonic frequencies defined by Eqn (3.7), which is essentially the ‘resonance’ condition for radiation fields (for this reason, transition radiation in a periodically inhomogeneous medium is referred to as resonance transition radiation [1]).

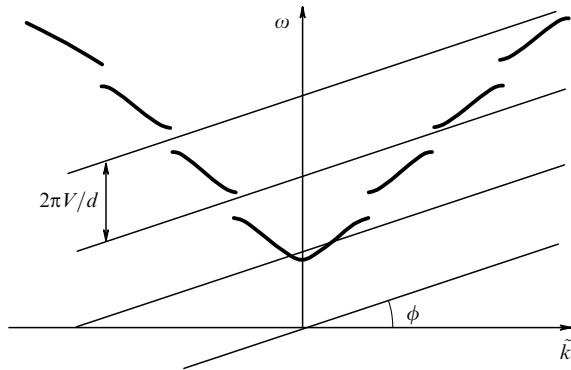


Figure 10. Graphical solution of the equation defining frequencies of emitted harmonics; $\tan \phi = V$.

The discrete nature of the radiation spectrum makes resonance possible in an elastic system when the group velocity of an emitted harmonic coincides with the load speed. Indeed, Fig. 10 shows that when one of the straight lines touches the dispersion curve (the group velocity $d\omega/dk$ coincides with load speed V), a real multiple root appears in Eqn (3.7), which leads to the divergency of integral (3.6). The possibility of resonance in an elastic periodically inhomogeneous system interacting with a moving load was first reported in Ref. [18].

Because the number of resonance velocities of the load is countable, this raises the problem of the effect of the support viscosity on the system oscillations at resonance and of the

identification of resonances ‘essential’ for practical purposes. Figure 11 shows the string displacement in the contact point versus the load speed ($\alpha = V/c$; the displacement is depicted at $t = 0$) for the parameters $\tilde{m} = m/\rho d = 0.15$, $\tilde{k} = kd/\rho c^2 = 10$, and $\tilde{\delta} = \delta/\rho c = 0.1$. Figures near the main resonance peaks denote frequencies of resonance harmonics whose group velocity at $\delta \rightarrow 0$ coincides with the load speed. An analysis of this dependence reveals that (1) the lower the resonance harmonic frequency, the weaker the effect of viscous supports on the amplitude of the corresponding resonance vibrations and the stronger the resonance, and (2) if the resonance harmonic frequencies are nearly identical (e.g., at $\alpha = 0.19$ and at $\alpha = 0.34$, $\omega_{\text{res}} \approx 2.25$), then the higher the speed of the load, the stronger the resonance. The first ‘selection rule’ for strong resonances rests on the enhancement of the support viscosity effect with growing vibration frequency, and the second one, on the rise in the transition radiation power with increasing load speed (it should be remembered that we consider the case of $V < c$).

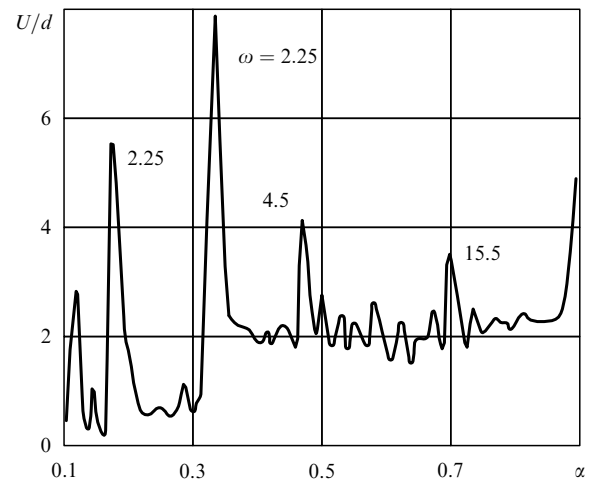


Figure 11. Speed dependence of the string displacement under the action of a moving load during its passage across the $n = 0$ support.

The emitted waves exert a pressure on the moving load (the horizontal component of the string reaction at the point of contact is nonzero). According to [20], the horizontal reaction of the string at the loading point (transition radiation, in the case under consideration) averaged over the spatial period is defined by the expression

$$\bar{F}_r = -\frac{P}{d} \int_0^d [U_x(Vt + 0, t) + U_x(Vt - 0, t)] dx. \tag{3.8}$$

The substitution of (3.6) into (3.8), calculation of the integral with respect to x , and introduction of a new integration variable $\tilde{\omega} = \omega c/d$ lead to

$$\frac{\bar{F}_r}{PF} = -\frac{\tilde{\delta}\alpha^2}{\pi(1-\alpha^2)} \int_0^\infty \left(\cos \frac{\tilde{\omega}}{\alpha} - \cos \tilde{\omega} \right) \tilde{\omega}^{-2} d\tilde{\omega} \times \left[\left(\cos \frac{\tilde{\omega}}{\alpha} - \cos \tilde{\omega} - \frac{\tilde{k} - \tilde{m}\tilde{\omega}^2}{2\tilde{\omega}} \sin \tilde{\omega} \right)^2 + \left(\frac{\tilde{\delta}}{2\tilde{\omega}} \sin \tilde{\omega} \right)^2 \right]^{-1}, \tag{3.9}$$

where $\alpha = V/c$, $\tilde{m} = m/\rho d$, $\tilde{k} = kd/\rho c^2$, $\tilde{\delta} = \delta/\rho c$. It follows from (3.9) that, on the average, the radiation reaction

decelerates the motion of the load. Figure 12 shows the dependence of the mean radiation reaction on the dimensionless viscosity of supports δ at various load speeds ($\tilde{m} = 0,15$, $\tilde{k} = 10$). It can be seen that at a high radiation power ($\alpha = 0.34$ corresponds to the resonance case, and $\alpha = 0.95$, to the load speed close to the wave propagation velocity in the string), the low viscosity of supports decreases the resistance to motion (radiation reaction). Otherwise ($\alpha = 0.4$), the resistance to motion grows slowly with increasing viscosity.

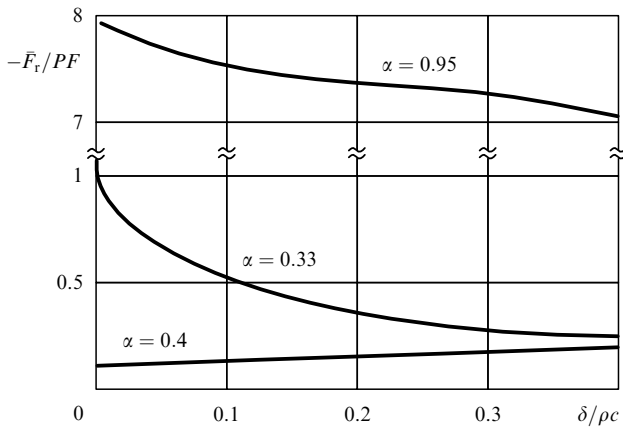


Figure 12. Dependence of the force of resistance to motion on the viscosity of supports.

To summarize, the transition radiation spectrum in a periodically inhomogeneous system is discrete. When the load speed and the group velocity of an emitted harmonic coincide, there is a marked increase in the amplitude of oscillations, i.e., resonance occurs. The radiation reaction is on the average different from zero, i.e., the moving load is subjected to a force of resistance to motion.

3.2 Motion of constant load along a closed periodically inhomogeneous elastic system (spoked wheels). Resonance conditions

An important example of a mechanical system in which a moving load can excite elastic waves is an elastic wheel, which is a standard element of most vehicles. If the wheel is non-uniform with respect to the angular coordinate, i.e., contains spokes, dampers, disk brakes, etc., transition radiation is likely to constitute one of the mechanisms of wave generation. Elucidation of such a mechanism is interesting from both theoretical and practical standpoints. Theoretically, specific features of the radiation process associated with the closed nature of an elastic system are of great interest, whereas the practical importance of the problem is related to a new type of railroad car wheels being currently designed (see above) and the need for development of a theory explaining ‘shimming’ (angular wheel vibrations of landing airplanes) with due regard for modern landing velocities.

A filament stretched by continuously distributed springs may serve as a wheel model (Fig. 13). Elastic inertial concentrated loads (‘spokes’) located equidistantly throughout the wheel length represent inhomogeneities of the elastic system. Let us assume that due to the interaction between the wheel and the earth surface (rail), the wheel is being subjected to a constant radial force P whose application point moves at a constant angular velocity $\Omega = \text{const}$. According to Ref. [20],

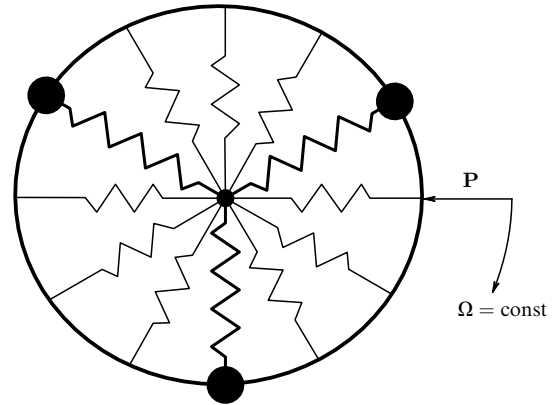


Figure 13. The uniform motion of a constant radial load along ‘a spoked wheel’.

the system of equations that describes small radial vibrations of such a filament has the form

$$\begin{aligned}
 U_{tt} - c^2 U_{ss} + h^2 U &= -\frac{P}{\rho} \delta\left(s - R\Omega t + l\left\{\frac{\Omega t}{2\pi}\right\}\right), \\
 0 \leq s \leq l, \quad 0 \leq t \leq \infty, \\
 [U]_{s=nl/N} &= 0, \quad U\left(\frac{nl}{N}, t\right) = U_n^0, \\
 T[U_s]_{s=nl/N} &= m\ddot{U}_n^0 + \delta\dot{U}_n^0 + kU_n^0, \quad U(s+l, t) = U(s, t).
 \end{aligned}
 \tag{3.10}$$

Here, $s = R\varphi$ is the angular coordinate; φ is the angle; R , the filament radius; l , the wheel length; N , the number of spokes; $1 \leq n \leq N$; $U(s, t)$ and $\ddot{U}_n^0(t)$ are the radial displacements of the string and the inertial element of the n th spoke, respectively; ρ , the mass per unit length of the filament; $c^2 = T/\rho$ is the radial wave velocity; T , the filament tension caused by the springs (see Ref. [23] for more details); $h^2 = k_0/\rho$; k_0 , the stiffness per unit length of the springs; m , δ , k are the spoke mass, viscosity, and stiffness, respectively (the length of the unexcited elastic element in a spoke is coincident with R); $\{b\}$ is the integer part of b ; and $[f]_{s=b} = f(b+0) - f(b-0)$.

The solution to (3.10) should be sought by the method of images, that is, on the assumption that the elastic system is boundless and subjected to additional fictitious loads in such a way as to satisfy both the closeness condition $U(s+l, t) = U(s, t)$ and the boundary conditions at the point of contact. Evidently, the field generated by loads P moving with speed ΩR at equal distances from one another meets these requirements. Hence, the auxiliary problem, the solution of which coincides with that of (3.10) at $s \in [0, l]$, can be written as

$$\begin{aligned}
 U_{tt} - c^2 U_{ss} + h^2 U &= -\frac{P}{\rho} \sum_{j=-\infty}^{\infty} \delta(s - Vt + jnd), \\
 -\infty \leq s \leq \infty, \quad -\infty \leq t \leq \infty, \\
 [U]_{s=nd} &= 0, \quad U(nd, t) = U_n^0, \\
 T[U_s]_{s=nd} &= m\ddot{U}_n^0 + \delta\dot{U}_n^0 + kU_n^0, \quad U(s+l, t) = U(s, t),
 \end{aligned}
 \tag{3.11}$$

where $V = \Omega R$ is the linear load speed and $d = l/N$ is the distance between the neighboring spokes at the wheel rim.

Steady state filament vibrations can be found by applying to (3.11) the integral Fourier transformation with respect to time (2.11). This leads to

$$\frac{\partial^2}{\partial s^2} V_\omega + \frac{1}{c^2}(\omega^2 - h^2)V_\omega = \frac{F}{V} \exp \frac{i\omega s}{V} \sum_{j=-\infty}^{\infty} \exp\left(\frac{i\omega d N}{V} j\right),$$

$$[V_\omega]_{s=nd} = 0, \quad V_\omega(nd, \omega) = V_{\omega n}^0(\omega),$$

$$T \left[\frac{\partial}{\partial s} V_\omega \right]_{s=nd} = (k - i\delta\omega - m\omega^2)V_{\omega n}^0(\omega), \quad (3.12)$$

where $V_\omega(s, \omega)$ and $V_{\omega n}^0(\omega)$ are the Fourier transforms of $U(s, t)$ and $U_n^0(t)$, respectively; and $F = P/\rho c^2$.

This problem is solved in the same way as described in Section 3.1 using the periodicity condition (3.4). Proceeding from the general condition at $s \in [0, d]$, we have

$$V_\omega = A \exp \frac{is\sqrt{\omega^2 - h^2}}{c} + B \exp\left(-\frac{is\sqrt{\omega^2 - h^2}}{c}\right) - S \exp \frac{i\omega s}{V},$$

$$S = \frac{FVc^2}{\omega^2(c^2 - V^2) + h^2V^2} \sum_{j=-\infty}^{\infty} \exp \frac{i\omega d N j}{V}. \quad (3.13)$$

The use of the periodicity condition leads to the expression for V_ω at arbitrary s

$$V_\omega = \exp \frac{i\omega s}{V} \left\{ A \exp \frac{i(s-d)\sqrt{\omega^2 - h^2}}{c} + B \exp\left[-\frac{i(s-d)\sqrt{\omega^2 - h^2}}{c}\right] \right\} - S \exp \frac{i\omega s}{V}. \quad (3.14)$$

Determining A and B by substituting (3.14) into the boundary conditions at $s = 0$ and $s = d$ [see (2.12)] and applying the inverse Fourier transformation to (3.13), we obtain the exact solution of (3.10) that describes steady-state filament vibrations at $s \in [0, d]$

$$U(s, t) = \frac{1}{2\pi} \int_{-\infty}^{\infty} \frac{S}{A} \left\{ Gp \left[(p - \gamma^-) \exp \frac{is\sqrt{\omega^2 - h^2}}{c} + (\gamma^+ - p) \exp\left(-\frac{is\sqrt{\omega^2 - h^2}}{c}\right) \right] - \Delta \exp \frac{i\omega x}{V} \right\} \times \exp(-i\omega t) d\omega, \quad (3.15)$$

where

$$\Delta = -\frac{4ip}{c} \sqrt{\omega^2 - h^2} \left[\cos \frac{\omega d}{V} - \cos\left(\frac{d}{c} \sqrt{\omega^2 - h^2}\right) - \frac{Gc}{2\sqrt{\omega^2 - h^2}} \sin\left(\frac{d}{c} \sqrt{\omega^2 - h^2}\right) \right],$$

$$p = \exp \frac{i\omega d}{V}, \quad \gamma^\pm = \exp\left(\pm \frac{id\sqrt{\omega^2 - h^2}}{c}\right),$$

$$G = \frac{k - i\delta\omega - m\omega^2}{T}.$$

The filament displacements in the interval of $s \in [d, Nd]$ are determined using the periodicity condition (3.3).

Similar to the case of motion along a boundless elastic system (Section 3.1), the load induces in the wheel radiation

with a discrete spectrum whose components have frequencies defined by Eqn (3.7) in which

$$\cos[\tilde{k}(\omega)d] = \cos \frac{d\sqrt{\omega^2 - h^2}}{c} + \frac{Gc}{2\sqrt{\omega^2 - h^2}} \sin \frac{d\sqrt{\omega^2 - h^2}}{c}. \quad (3.16)$$

Eqn (3.16) is the dispersion equation for a spring-supported string resting on periodical supports.

Let us now consider the resonance parameters of the system responsible for a sharp rise in the wheel vibration amplitude, which is of great practical importance. Without the loss of generality, we first find resonance conditions by examining the amplitude of steady-state vibrations of a spoke. For the sake of brevity, we will consider the spoke $n = 0$ and calculate its displacement at $t = 0$ (the choice of time is immaterial in resonance studies of steady-state vibrations, provided the displacement is nonzero). According to (3.15), the displacement of the inertial element of the selected spoke at $t = 0$ is defined by the expression

$$U_0^0(0) = -\frac{1}{4\pi} \int_{-\infty}^{\infty} S \frac{\cos(\omega d/V) - \cos(d\sqrt{\omega^2 - h^2}/c)}{\cos(\omega d/V) - \cos[\tilde{k}(\omega)d]} d\omega, \quad (3.17)$$

where $\cos[\tilde{k}(\omega)]$ is defined by (3.16).

Calculating integral (3.17) by the residue calculus methods (see [22] for the detailed description of the calculations), we obtain

$$U_0^0(0) = -\frac{I_1 + I_2 + I_3}{4\pi},$$

$$I_1 = \pi i \sum_m \operatorname{res}_{\operatorname{Im}(\omega_m) > 0} \left[D^{-1}(\omega_m) \times \left(\exp \frac{i\omega_m d}{V} - \exp \frac{id\sqrt{\omega_m^2 - h^2}}{c} \right) \right]$$

$$- \pi i \sum_l \operatorname{res}_{\operatorname{Im}(\omega_l) < 0} \left[D^{-1}(\omega_l) \times \left(\exp \frac{i\omega_l d}{V} - \exp \frac{id\sqrt{\omega_l^2 - h^2}}{c} \right) \right]$$

$$- \int_{-1}^1 D^{-1} \sinh \frac{d\sqrt{\omega^2 - h^2}}{c} d\omega,$$

$$I_2 = 2\pi i \sum_m \frac{\exp(i\omega_m d N/V)}{1 - \exp(i\omega_m d N/V)} \times \operatorname{res}_{\operatorname{Im}(\omega_m) > 0} \left[D^{-1}(\omega_m) \left(\exp \frac{i\omega_m d}{V} - \exp \frac{id\sqrt{\omega_m^2 - h^2}}{c} \right) \right],$$

$$I_3 = -2\pi i \sum_l \frac{\exp(-i\omega_l d N/V)}{1 - \exp(-i\omega_l d N/V)} \times \operatorname{res}_{\operatorname{Im}(\omega_l) < 0} \left[D^{-1}(\omega_l) \left(\exp \frac{i\omega_l d}{V} - \exp \frac{id\sqrt{\omega_l^2 - h^2}}{c} \right) \right],$$

$$D(\omega) = \left\{ \cos \frac{\omega d}{V} - \cos[\tilde{k}(\omega)d] \right\} \frac{\omega^2(c^2 - V^2) + h^2V^2}{FVc^2}, \quad (3.18)$$

where ω_m and ω_l are zeros of the $D(\omega)$ function of the complex variable ω on the upper and lower half-planes,

respectively, and $\text{res}\{f(\omega_k)\}$ is the residue of the function $f(\omega)$ at point $\omega = \omega_k$. It follows from (3.18) that resonance (i.e. the tending of the spoke displacement to infinity when its viscosity δ tends to zero) is likely to occur in the following two cases: (a) Eqn $D(\omega) = 0$ at $\delta \rightarrow 0$ has a multiple real root, with the residue at this point tending toward infinity and (b) the root of the equation $D(\omega) = 0$ at $\delta \rightarrow 0$ coincides with one of the roots of the equation $1 - \exp(\pm i\omega dN/V) = 0$, with either I_2 or I_3 tending to zero.

Physically, case (a) means that the group velocity of one of the harmonics radiated is coincident with the load speed. In boundless systems, unlike bounded ones (see Section 3.1), this condition is actually the single resonance condition. However, this is not the case in closed systems unless the emitted wave length is divisible by the wheel length. It was shown in Ref. [22] that if condition (a) is met, each of the summands in (3.18) diverges, but their summation gives a finite result.

As for case (b), it actually defines the parameters of the system that are responsible for resonance. Mathematically, this is trivial, because $U_0^0(0)$ here tends to infinity due to the growth of one of the summands. From the physical point of view, condition (b) is sufficiently transparent. Indeed, the real roots of equation $D(\omega) = 0$, which can be rewritten (for real roots) in the form

$$\tilde{k}(\omega) + \frac{2\pi m}{d} = \frac{\omega}{V}, \quad m = 0, \pm 1, \pm 2, \dots, \quad (3.19)$$

define the frequencies of load-excited harmonics. The roots of the equations $1 - \exp(\pm i\omega dN/V) = 0$, which are coincident with the roots of the equation

$$\sin \frac{\omega dN}{2V} = \sin \frac{\pi\omega}{\Omega} = 0,$$

correspond to wheel vibrations with frequencies ω , which are integer multiples of the frequency of the load rotation Ω

$$\omega_l = l\Omega, \quad l = 0, \pm 1, \pm 2, \dots \quad (3.20)$$

Thus, resonance in a spoked wheel occurs when the frequency of the load rotation is divisible by the frequency of one of the emitted harmonics. The resonance condition can also be written in another form. Substitution of (3.20) into (3.19) yields

$$m\lambda_m = Nd,$$

where $\lambda_m = 2\pi/(\tilde{k} + 2\pi m/d)$ is the wavelength of the m th emitted harmonic. This indicates that resonance may occur when the wheel length is divisible by the wavelength of one of the emitted harmonics.

The graphical solution of the system (3.19), (3.20) is presented in Fig. 14. The broken line is the dispersion curve $\tilde{k}(\omega)$ of a periodically inhomogeneous system (a split representation of the wheel rim). The intersections between a family of monotonically sloping curves $\omega_m = \tilde{k}(\omega)V + 2\pi Vm/d$ and the curve $\tilde{k}(\omega)$ define the frequencies of the load-induced harmonics. Resonance occurs when ω_m coincides with, or is a multiple of, the load rotation frequency Ω ($\omega_l = l\Omega$ is a family of horizontal straight lines). Graphically, resonance takes place when the dispersion curve intersects with two straight lines (one horizontal and one sloping) at one point.

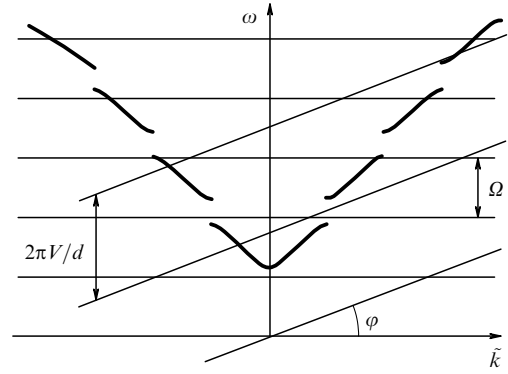


Figure 14. Graphical solution of the system responsible for the resonance parameters of a wheel; $\tan \varphi = V$.

Figure 15 presents a family of curves on the plane of dimensionless parameters (hd/c ; V/c) characterizing the possibility of resonance when the parameters of the system fall onto these curves (calculations were made on the assumption that $kc/hT = 0.7$, $\delta c/T = 0$, $mhc/T = 0.3$, $N = 2$). In reality, the figure shows only part of the solutions to the system (3.19), (3.20) (there is a countable number of them), namely, the curves corresponding to frequencies that are no more than 3 times the load's rotational frequency. There is no sense in considering higher frequencies because the corresponding resonances are most likely to be suppressed by dissipation inherent in all real wheels. At the intersections between each curve and the straight line $V/c = 1$, double indices (m, l) are given; the first figure shows how many times higher the resonance frequency is than the load rotation frequency; the second figure corresponds to the order number of the harmonic emitted. Also, Fig. 15 shows that the 'resonant' distance between the spokes increases with an increase in load speed. Note that there are zones of concentration of resonance parameters of the system (for instance, at $V/c \approx 0.8$ and $hd/c \approx 1$).

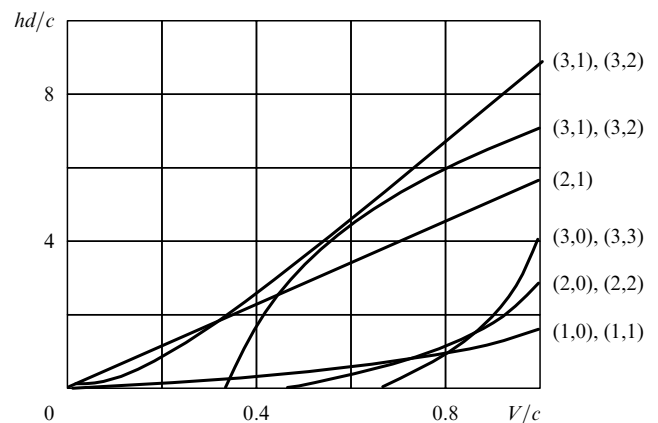


Figure 15. A family of curves characterizing the possibility of resonance to occur in a wheel when the system's parameters fall on them.

To select 'strong' resonances, one should follow the same rule as that for the motion along a boundless system (Section 3.1), that is, the lower the resonance frequency and the higher the load speed, the stronger the resonance.

3.3 Motion of mass along a string resting on a periodically inhomogeneous elastic foundation.

Parametric instability of vibrations

If the perturbation source has its own degrees of freedom, the radiation emitted may increase its internal energy [14]. This is the case when the object emits anomalous Doppler waves. Anomalous waves in elastic systems may generate unstable vibrations of moving objects [15–17]. Periodically inhomogeneous systems are known to have a decelerating effect. Therefore, it is natural to expect that objects moving in such systems will experience unstable oscillations even at ‘subcritical’ speeds (lower than the maximum rate of energy transfer). Another (‘mechanical’) line of reasoning is also worthy of note. Imagine an object that uniformly moves along an elastic guide resting on an elastic foundation, with the stiffness of the foundation periodically changing in space. The spring rigidity under the moving object also varies periodically (in time) due to the uniformity of motion and the periodicity of the guide parameters. Therefore, vibrations of an object moving along the guide are equivalent to its vibrations on a spring with periodically changing rigidity (Fig. 16). Evidently, such a situation may lead to parametric instability of the object vibrations.

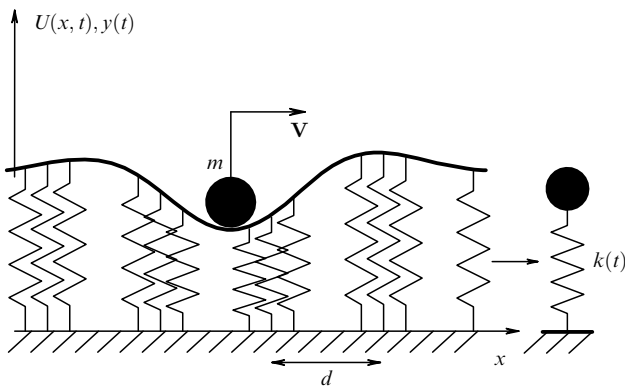


Figure 16. The motion of a mass along a string resting on a periodically inhomogeneous foundation. In the right-hand side of the figure, an equivalent model is shown, i.e., a mass supported by a spring with rigidity periodical in time.

It is this instability that is responsible for the ‘galloping’ of train wheels and sparking in the electric traction system.

In order to analyze conditions for the appearance of parametric resonance, let us consider the uniform ($x = Vt$) motion of mass m along a boundless string resting on an elastic foundation (see Fig. 16) whose stiffness per unit length is described by the expression

$$k(x) = k_0 \left(1 + \mu \cos \frac{2\pi x}{d} \right),$$

where k_0 is the mean stiffness, d is the inhomogeneity period, and $\mu \ll 1$ is a dimensionless small parameter. For simplicity, we assume that the system is not affected by external vertical forces, because they do not interfere with its stability by virtue of the problem’s linearity. According to Ref. [22], the problem describing mass and string vibrations without loss of contact may be written as follows:

$$U_{tt} - c^2 U_{xx} + h^2(x)U = -\frac{m}{\rho} \ddot{U}_0 \delta(x - Vt),$$

$$U_0(t) = U(Vt, t), \quad -\infty < x, t < \infty, \quad c^2 = \frac{N}{\rho},$$

$$h^2(x) = \frac{h_0^2}{\rho} \left(1 + \mu \cos \frac{2\pi x}{d} \right), \quad h_0^2 = \frac{k_0}{\rho}, \quad (3.21)$$

where $U(x, t)$ and $U_0(t)$ are the vertical string and mass displacements, respectively; ρ and N are the mass per unit length and the tension of the string; and the velocity of the mass is assumed to be subcritical, i.e., $V < c$.

The solution to (3.21) can be obtained based on the theory of perturbations in the form

$$U = U^{(0)} + \mu U^{(1)} + \dots, \quad U_0 = U_0^{(0)} + \mu U_0^{(1)} + \dots \quad (3.22)$$

In the zero approximation ($\mu = 0$), (3.21), (3.22) reduce to the problem of mass motion along a string lying on a homogeneous elastic foundation with stiffness k_0

$$U_{tt}^{(0)} - c^2 U_{xx}^{(0)} + h_0^2 U^{(0)} = -\frac{m}{\rho} \frac{d^2}{dt^2} [U_0^{(0)}(t)] \delta(x - Vt),$$

$$U_0^{(0)}(t) = U^{(0)}(Vt, t).$$

Using the fundamental solution for the operator

$$\frac{\partial^2}{\partial t^2} - c^2 \frac{\partial^2}{\partial x^2} + h_0^2,$$

in the form of

$$J_0 \left(\frac{h_0}{c} \sqrt{c^2 t^2 - x^2} \right) \frac{\Theta(ct - |x|)}{2c}$$

(J_0 is the zero-order Bessel function, and Θ is the unit function), the expression for $U^{(0)}(x, t)$ may be written as

$$U^{(0)}(x, t) = -\frac{m}{2\rho c} \int_0^t \frac{d^2}{d\tau^2} [U_0^{(0)}(\tau)] \times J_0 \left[\frac{h_0}{c} \sqrt{c^2(t - \tau)^2 - (x - V\tau)^2} \right] \Theta(t - \tau - |x - V\tau|) d\tau.$$

Using now the no-loss-of-contact condition for mass and string vibrations, we obtain an expression for describing vertical mass vibrations on the string (note that $V < c$)

$$U_0^{(0)}(t) + \frac{m}{2\rho c} \int_0^t \frac{d^2}{d\tau^2} [U_0^{(0)}(\tau)] J_0 \left[\frac{h_0}{c} \sqrt{c^2 - V^2}(t - \tau) \right] d\tau = 0. \quad (3.23)$$

Seeking the solution to (3.23) in the form $U_0^{(0)}(t) = A \exp i\tilde{\Omega}t$ and tending t to ∞ , we obtain an expression that defines the vibration frequency of the mass moving along the string at $t \rightarrow \infty$

$$1 - \frac{M\Omega^2}{2\sqrt{1 - \alpha^2 - \Omega^2}} = 0, \quad M = \frac{mh_0}{\rho c}, \quad \Omega = \frac{\tilde{\Omega}}{h_0}, \quad \alpha = \frac{V}{c},$$

from which we have

$$\Omega = \pm \frac{\sqrt{2}}{M} \sqrt{[1 + M^2(1 - \alpha^2)]^{1/2} - 1}. \quad (3.24)$$

Therefore, vibrations of a mass uniformly moving along a string resting on a homogeneous elastic foundation at $t \rightarrow \infty$ are actually harmonic oscillations (Ω is real) described by the equation

$$U_0^{(0)}(\tau) = A \exp i\Omega\tau + B \exp(-i\Omega\tau),$$

$$\tau = h_0 t, \quad t \rightarrow \infty. \tag{3.25}$$

The expression for string vibrations corresponding to mass vibrations at $t \rightarrow \infty$ can easily be derived in the form of superposition of ‘plane’ waves (τ, z are the dimensionless time and coordinate, respectively):

$$U^{(0)} = C_1 \exp(i\omega_j\tau - ik_jz) + C_2 \exp(i\omega_{j+2}\tau - ik_{j+2}z),$$

$$z = \frac{xh}{c}, \quad j = \begin{cases} 1, & z < \alpha\tau, \\ 2, & z > \alpha\tau, \end{cases}$$

$$k_{1,2} = \frac{\alpha\Omega \pm i\sqrt{1 - \alpha^2 - \Omega^2}}{\sqrt{1 - \alpha^2}}, \quad \omega_{1,2} = \alpha k_{1,2} + \Omega,$$

$$k_{3,4} = -\frac{\alpha\Omega \pm i\sqrt{1 - \alpha^2 - \Omega^2}}{\sqrt{1 - \alpha^2}}, \quad \omega_{3,4} = \alpha k_{3,4} - \Omega,$$

$$C_1 = \frac{A\Omega^2}{2\sqrt{1 - \alpha^2 - \Omega^2}}, \quad C_2 = \frac{B\Omega^2}{2\sqrt{1 - \alpha^2 - \Omega^2}}. \tag{3.26}$$

Thus, a mass on a homogeneous string undergoes harmonic vibrations. It is therefore natural to expect that taking into account periodic inhomogeneity of the elastic foundation leading to periodical-in-time (with a period $T = d/V$) changes of string rigidity under the moving mass may give rise to parametric resonance with the first instability zone occurring under the condition that

$$2\Omega = \alpha\chi + \mu\delta, \tag{3.27}$$

where $\alpha\chi$ ($\alpha = V/c, \chi = 2\pi c/hd$) is the dimensionless frequency with which the stiffness of the elastic foundation varies beneath the moving mass and δ is the dimensionless detuning.

It was demonstrated in Ref. [22] that parametric resonance can occur in reality in the system under examination. The paper provides a detailed description of the procedure intended to seek out the boundaries of the first instability zone by analogy with the standard method employed in the analysis of parametric resonance in concentrated systems (see Refs [24, 25]). Using this approach, the solution to (3.21) is sought in the form of a series (3.22), but in the zero approximation (3.25), (3.26), the amplitudes are assumed to be slowly varying (because the system is continuous, the amplitudes must change both in time and space), and a small detuning is introduced in the phase:

$$U_0(\tau) = A(\mu\tau) \exp[i\tau(\Omega + \mu\delta)] + B(\mu\tau) \exp[-i\tau(\Omega + \mu\delta)] + \mu U_0^{(1)}(\tau) + \dots,$$

$$U(z, \tau) = C_1^j(\mu z, \mu\tau) \exp[i\tau(\omega_j + \mu\delta) - ik_j z] + C_2^j(\mu z, \mu\tau) \exp[i\tau(\omega_{j+2} + \mu\delta) - ik_{j+2} z] + U^{(1)}(z, \tau) + \dots \tag{3.28}$$

The equation for the boundaries of the zone of instability is obtained from the condition that $U_0^{(1)}(\tau)$ and $U^{(1)}(z, \tau)$ must not grow in time [series (3.28) must be asymptotically

convergent], and has the form

$$\alpha\chi - 2\Omega \pm \mu \frac{\alpha^2\Omega(1 - \alpha^2)^2}{16(\alpha^2 + \Omega^2)(1 + 2/M^2\Omega^2)} = 0. \tag{3.29}$$

Note that the dimensionless quantities in (3.29) have the following meaning: α is the mass velocity, χ is the wave number of inhomogeneity, M is the mass, and Ω is the oscillation frequency of the mass moving along a string that rests on a homogeneous foundation [defined by (3.24)].

Figure 17 shows instability zones for different χ obtained in accordance with (3.29). It is inferred from an analysis of these graphs that (a) the smaller the inhomogeneity period (the larger χ), the lower the velocities at which the instability occurs, (b) the mass necessary to induce the instability decreases with an increase in velocity, (c) the instability zone expands in α with an increase in mass and (or) inhomogeneity period. It should be emphasized that the boundaries of the instability zone (3.29) thus found are the boundaries of the main instability zone obtained in the first approximation in the small parameter μ .

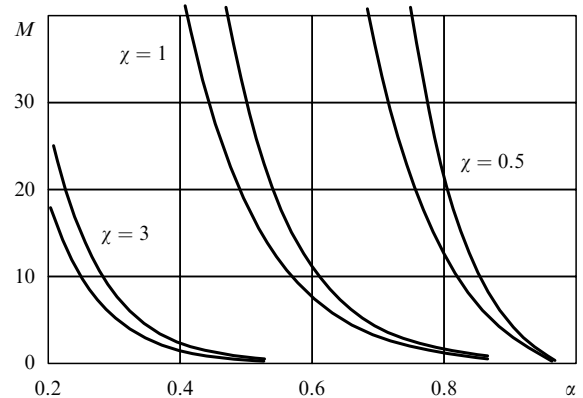


Figure 17. The main zone of mass oscillation instability for different inhomogeneity periods of a stiff foundation.

An important issue is the effect of small viscosity of the elastic foundation on the solution of the problem in question. With viscosity taken into consideration, the first equation in (3.21) assumes the form ($\mu\nu$ is the low viscosity of the foundation)

$$U_{tt} - c^2 U_{xx} + 2\mu\nu U_t + h^2(x)U = -\frac{m}{\rho} \ddot{U}_0\delta(x - Vt),$$

while the following inequality stands for the instability condition:

$$\frac{M^2\Omega^4(1 - \alpha^2)^2}{16(\alpha^2 + \Omega^2)^2(v^2 + 16\Omega^2/\alpha^4)} - \delta^2 \left(M + \frac{2}{M\Omega^2} \right)^2 - \frac{4v^2}{M^2\Omega^4} > 0, \quad \delta = \frac{\alpha\chi - 2\Omega}{\mu}. \tag{3.30}$$

Figure 18 depicts the instability zones obtained according to (3.30) at $v = 0.7$. There is a region in the space of system’s parameters (the one below the dashed curve) where oscillations are stable at any inhomogeneity period. Interestingly, the effect of elastic foundation viscosity grows as mass velocity increases.

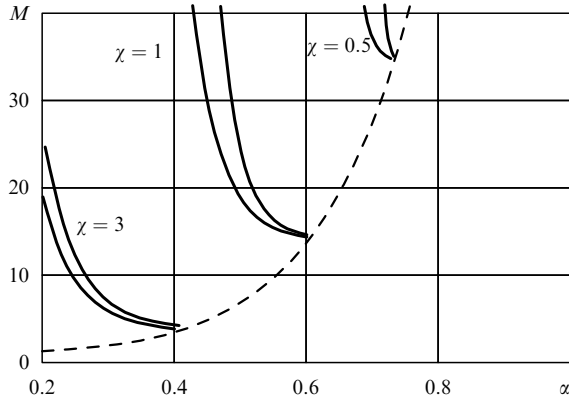


Figure 18. The main instability zone, with the viscosity of the string foundation taken into account.

In summary, the uniform motion of a mass (or an arbitrary object) in a periodically inhomogeneous elastic system is accompanied by parametric resonance which appears as an exponential growth of the amplitude of mass vibrations. It has already been mentioned that the work necessary to increase the energy of mass vibrations is performed by an external source that maintains the uniform motion.

Mass vibrations were examined in an elastic system without loss of contact. However, the wheels of a real train can lose contact with the rails for a time and then regain contact (‘galloping’). The fact that the parameters of the above problem belong to the stability region does not necessarily suggest that the motion of an object occurs without loss of contact. However, if these parameters fall into the instability region, the loss of contact at $t \rightarrow \infty$ is unavoidable, i.e., it is a sufficient condition for ‘galloping’.

4. Transition radiation in randomly inhomogeneous one-dimensional elastic systems

The assumption of regular properties of real elastic guides is a controversial issue. Indeed, the crossties on which a railroad track is laid are not strictly periodical, the distance between wire clamps is variable (up to a few percent), and the track ballast is a random structure. It is therefore necessary to answer the question of whether the allowance for spatial fluctuations of the parameters of the elastic systems under consideration can lead to qualitative changes in their dynamic behavior (during transition radiation, in particular) or not. There are many reasons for giving a positive answer. For instance, transition radiation in randomly inhomogeneous guides is incoherent, unlike that in periodic systems. A more essential question, however, is appropriate: whether real structures must be strictly periodic or small fluctuations are conducive to the attenuation of dynamic stress. These questions are discussed below.

The discussion is of a twofold nature. Let us first suppose that a load moves along a randomly inhomogeneous system and examine resonance vibrations of this system during transition radiation, which are crucial for practical reasons. Then, we consider inertia of a moving object and demonstrate the possibility of stochastic parametric resonance in a randomly inhomogeneous elastic system subjected to such an object. These problems are not classical in the field of

transition radiation studies, but our objective is to focus on specific features of transition radiation in mechanical systems and avoid reiterating electrodynamic and acoustic results [1, 5].

4.1 Motion of constant load along a string resting on a randomly inhomogeneous elastic foundation. Limitations on the amplitude of resonance oscillations, average radiation reaction

If a randomly inhomogeneous guide is subjected to a moving load, the waves emitted at each inhomogeneity are unable to interfere in a resonance manner because the inhomogeneities are irregular. As a result, the radiation is localized near the moving load, which makes radiation in a randomly inhomogeneous medium similar to the process of wave formation in a dissipative medium, where the emitted waves are attenuated. Interestingly, classical effects that can arise due to dissipation in a moving load–elastic guide system, such as limitation on the resonance oscillation amplitude and the resistance to load motion [26], are also observed when the load moves along a randomly inhomogeneous guide. This is natural, since emitted waves are equivalent to dissipation from the load’s ‘point of view’, for they take away energy from the load and the radiation reaction hinders its motion due to the ‘recoil effect’.

To illustrate the above reasoning, let us consider the uniform motion of a vertical load $P \exp i\Omega t$ along a string resting on an elastic foundation with rigidity per unit length

$$k(x) = k_0 + \frac{1}{2} \mu k_1(x), \tag{4.1}$$

where $k_0 = \text{const}$, $\mu \ll 1$ is the dimensionless small parameter, $k_1(x)$ is the random coordinate function, and $\langle k_1(x) \rangle = 0$. Angular brackets $\langle \dots \rangle$ indicate statistical averaging. The load is assumed to be oscillating, in order to demonstrate the effect of limitation on resonance oscillations at subcritical velocities. The load being constant, the first ‘resonance velocity’ is wave velocity in the string and the motion at this speed is a separate complex problem that lies beyond the scope of this paper.

The vertical string displacement caused by the load is described by the following system of equations:

$$\begin{aligned} U_{tt} - c^2 U_{xx} + h^2(x)U &= -\frac{P}{\rho} \exp i\Omega t \delta(x - Vt), \\ -\infty < x, t < \infty, \quad c^2 &= \frac{N}{\rho}, \\ h^2(x) &= h_0^2 + \mu h_1(x), \quad h_0^2 = \frac{k_0}{\rho}, \quad h_1(x) = \frac{k_1(x)}{\rho}, \end{aligned} \tag{4.2}$$

where $U(x, t)$ is the vertical displacement of the string; N and ρ are its tension and the mass per unit length, respectively; the motion of the load is assumed to be subcritical, i.e., $V < c$.

The problem (4.2) can be analyzed using the mean field method [27, 28]. A disadvantage of this method lies in the loss of information about the oscillation phase, but it is immaterial for our purpose (analysis of the vibration amplitude at resonance and estimation of the average radiation reaction).

The application to (4.2) of the integral Fourier transformation with respect to time (2.11) yields

$$\frac{\partial^2}{\partial x^2} V_\omega + \frac{1}{c^2} [\omega^2 - h^2(x)] V_\omega = \frac{F}{V} \exp\left(i \frac{\omega + \Omega}{V} x\right),$$

$$F = \frac{P}{\rho c^2}. \tag{4.3}$$

According to the mean field method, we must seek the solution to (4.3) as the sum of the mean field $\langle V_\omega \rangle$ and a fluctuation field V_ω^1 for which $\langle V_\omega^1 \rangle = 0$:

$$V_\omega = \langle V_\omega \rangle + \mu V_\omega^1. \tag{4.4}$$

The substitution of (4.4) into (4.3) yields the following equation:

$$\begin{aligned} \frac{\partial^2}{\partial x^2} (\langle V_\omega \rangle + \mu V_\omega^1) + \frac{1}{c^2} [\omega^2 - h_0^2 - \mu h_1(x)] (\langle V_\omega \rangle + \mu V_\omega^1) \\ = \frac{F}{V} \exp\left(i \frac{\omega + \Omega}{V} x\right), \end{aligned} \tag{4.5}$$

which is converted to the equation for the mean field of string vibrations by statistical averaging

$$\begin{aligned} \frac{\partial^2}{\partial x^2} \langle V_\omega \rangle + \frac{1}{c^2} (\omega^2 - h_0^2) \langle V_\omega \rangle - \mu^2 \frac{1}{c^2} \langle h_1(x) V_\omega^1 \rangle \\ = \frac{F}{V} \exp\left(i \frac{\omega + \Omega}{V} x\right). \end{aligned} \tag{4.6}$$

The equation for the fluctuation field is obtained by subtracting (4.6) from (4.5) and using only the μ -order terms:

$$\frac{\partial^2}{\partial x^2} V_\omega^1 + \frac{1}{c^2} (\omega^2 - h_0^2) V_\omega^1 = \frac{1}{c^2} \langle V_\omega \rangle h_1(x). \tag{4.7}$$

The Green's function of Eqn (4.7) has the form [26, 29]

$$\begin{aligned} \varphi(|x|, \omega) &= \frac{1}{2ia(\omega)} \exp[ia(\omega)|x|], \\ a(\omega) &= \frac{1}{c} \begin{cases} +\sqrt{\omega^2 - h_0^2}, & \omega > h_0, \\ i\sqrt{h_0^2 - \omega^2}, & |\omega| < h_0, \\ -\sqrt{\omega^2 - h_0^2}, & \omega < -h_0. \end{cases} \end{aligned}$$

Hence, the fluctuation field is related to the mean field in the following way:

$$V_\omega^1(x, \omega) = \frac{1}{c^2} \int_{-\infty}^{\infty} \langle V_\omega(\xi, \omega) \rangle h_1(\xi) \varphi(|x - \xi|, \omega) d\xi. \tag{4.8}$$

The substitution of relation (4.8) into (4.6) leads to a closed equation for the mean field of string displacements (in Fourier images):

$$\begin{aligned} \frac{\partial^2}{\partial x^2} \langle V_\omega \rangle + \frac{1}{c^2} (\omega^2 - h_0^2) \langle V_\omega \rangle \\ - \mu^2 \frac{1}{c^2} \int_{-\infty}^{\infty} \langle V_\omega(\xi, \omega) \rangle K(x, \xi) \varphi(|x - \xi|, \omega) d\xi \\ = \frac{F}{V} \exp\left(i \frac{\omega + \Omega}{V} x\right), \end{aligned} \tag{4.9}$$

where $K(x, \xi) = \langle h_1(x) h_1(\xi) \rangle$ is the inhomogeneity correlation function.

Henceforth, we will consider the fluctuations to be uniform, i.e., $K(x, \xi) = K(|x - \xi|)$. This assumption allows for the introduction of an effective stiffness of an elastic foundation (analog of effective permittivity [27]). Indeed, applying the integral Fourier transformation with respect to the coordinate to (4.9)

$$\langle W_{\omega,k}(k, \omega) \rangle = \int_{-\infty}^{\infty} \langle V_\omega(x, \omega) \rangle \exp(-i\chi x) dx,$$

we obtain

$$\begin{aligned} \langle W_{\omega,k} \rangle &= \frac{2\pi F}{V} \delta\left(\frac{\omega + \Omega}{V} - \chi\right) \\ &\times \frac{1}{-\chi^2 + (\omega^2 - h_0^2)/c^2 - \mu^2 H(\omega, \chi)}, \end{aligned} \tag{4.10}$$

where

$$H(\omega, \chi) = 2 \int_0^{\infty} K(\xi) \varphi(\xi) \cos \chi \xi d\xi$$

is the effective stiffness of the elastic foundation of the string.

Similar to frequency-dependent dissipation, the effective stiffness of an elastic foundation is non-invariant with respect to the substitution $\omega \rightarrow -\omega$ [due to the non-invariance of $\varphi(\xi, \omega)$ and accounts for the absence of (simultaneously) both real ω and real χ converting the dispersion equation

$$-\chi^2 + \frac{\omega^2 - h_0^2}{c^2} - \mu^2 H(\omega, \chi) = 0$$

to the identity. These properties of effective stiffness are responsible for the limited string displacement upon resonance and the resistance to motion. Indeed, the application to (4.10) of the inverse Fourier transformations with respect to time and coordinate yields

$$\begin{aligned} \langle U(x, t) \rangle &= \frac{F}{2\pi V} \int_{-\infty}^{\infty} \exp[ix(\omega + \Omega)/V - i\omega t] \\ &\times \left[-\frac{(\omega + \Omega)^2}{V^2} + \frac{\omega^2 - h_0^2}{c^2} - \mu^2 H\left(\omega, \frac{\omega + \Omega}{V}\right) \right]^{-1} d\omega. \end{aligned} \tag{4.11}$$

Because no real frequency and wave number (the roots of the dispersion equation) are present simultaneously, the denominator in (4.11) does not vanish on a set of real ω and the integral is convergent at all system parameters. Were the elastic foundation homogeneous ($\mu = 0$), the denominator in (4.11) would have a real multiple root, provided the resonance condition $V = c(1 - \Omega^2/h_0^2)^{1/2}$, $\Omega < h_0$ is met.

As regards the statistically mean force of resistance to motion F^r , it differs from zero even at $\Omega = 0$. This follows from the expression for $\langle F^r \rangle$ (see below), which is obtained using (4.11) and the general expression for the horizontal component of the string reaction for the load being examined ($\Omega = 0$):

$$\begin{aligned} F^r &= -P \exp i\Omega t [U_x(Vt - 0, t) + U_x(Vt + 0, t)]: \\ \langle F^r \rangle &= -\frac{F}{2\pi V} \int_{-\infty}^{\infty} \frac{i\omega \{ \exp[i\omega \times (-0)] + \exp[i\omega \times (+0)] \}}{-\omega^2 + V^2(\omega^2 - h_0^2)/c^2 - \mu^2 V^2 H(\omega, \omega/V)} d\omega. \end{aligned}$$

$\langle F^r \rangle$ can be calculated by contour integration. The first and second terms of the integrand [the exponent of the argument is multiplied by (-0)] must be integrated over the lower and upper half-planes of the complex variable ω , respectively. The integration of these terms leads to different results because the denominator of the integrand is non-invariant with respect to the substitution $\omega \rightarrow -\omega$. Hence, $\langle F^r \rangle \neq 0$. Specifically, if the inhomogeneity is delta-correlated [$K(x) = \delta(x)$], then $\langle F^r \rangle$ is described by the following expression:

$$\langle F^r \rangle = -\mu^2 \frac{V^2 P^2}{4\rho c^3 \sqrt{c^2 - V^2}}.$$

Thus, a random inhomogeneity of the guide restricts the amplitude of its resonance oscillations excited by the moving object. Therefore, it is tempting to infer that an irregular structure of the guide is always preferable (to reduce vibrations) than periodic inhomogeneity because it introduces additional effective dissipation in the system. However, this conclusion is incorrect, as becomes evident when we take into consideration coupled vibrations of the moving object and the elastic system. It will be shown in the next section that the regions of unstable vibrations of an object moving along a randomly inhomogeneous guide may be much broader than they are when the same object moves in a periodic elastic system. Therefore, the parameters of random inhomogeneities must be selected very carefully to avoid radiation-induced vertical ‘swinging’ of the object.

4.2 Motion of mass along a string resting on a randomly inhomogeneous elastic foundation. Stochastic parametric resonance

It was shown in Section 3.3 that oscillations of a mass moving uniformly along a periodically inhomogeneous elastic system are equivalent to vibrations of the same mass on a spring with rigidity periodically changing in time. It is clear that a mass on a spring whose rigidity randomly changes in time may serve as an equivalent model describing vibrations of a mass moving along a randomly inhomogeneous guide. It is known [30, 31] that mass vibrations at such a spring may be unstable because of stochastic parametric resonance. Hence, instability zones must also exit in the space of the parameters of the moving mass – randomly inhomogeneous guide system.

To verify the above proposition, we will analyze (Fig. 19) the uniform ($x = Vt$) motion of a mass m along a string with mass per unit length ρ and tension N that lies on a randomly inhomogeneous elastic foundation with stiffness per unit length $k(x) = k_0 + \mu k_1(x)/2$ [see expression (4.1)]. Let us

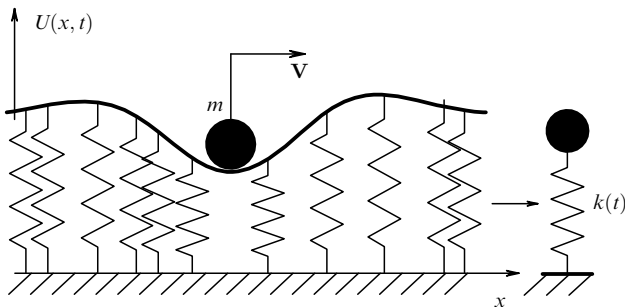


Figure 19. The motion of a mass along a string on a randomly inhomogeneous foundation. The equivalent model: a mass supported by a string with rigidity randomly varying in time.

introduce the following dimensionless variables and parameters: $z = xh_0/c$, $\tau = h_0 t$ ($c^2 = N/\rho$, $h_0^2 = k_0/\rho$) for the coordinate and the time; $\alpha = V/c$ ($\alpha < 1$) for the mass speed; and $M = mh_0/\rho c$ for the mass; $h_1(z) = k_1(z)/k_0\rho$ is represented as

$$h_1(z) = \int_{-\infty}^{\infty} Q(\chi) \exp i\chi z \, d\chi = \int_{-\infty}^{\infty} Q^*(\chi_1) \exp(-i\chi_1 z) \, d\chi_1,$$

$$\langle Q(\chi) \rangle = \langle Q^*(\chi_1) \rangle = 0. \quad (4.12)$$

Now, we assume again that the fluctuations are uniform, i.e.,

$$\langle h_1(z)h_1(z_1) \rangle = K(|z - z_1|) \Leftrightarrow \langle Q(\chi)Q^*(\chi_1) \rangle = S(\chi)\delta(\chi - \chi_1),$$

where $K(z)$ and $S(\chi)$ are the correlation function and its spectrum interrelated via Wiener – Khintchine relations.

The equations for mass and string vibrations that cause no loss of contact will be written in a moving coordinate system $\xi = z - \alpha\tau$, bearing in mind (4.12) (see Ref. [32] for more details):

$$U_{\tau\tau} - 2\alpha U_{\tau\xi} - (1 - \alpha^2)U_{\xi\xi} + 2\mu\nu(U_{\tau} - \alpha U_{\xi}) + U \left\{ 1 + \mu \int_{-\infty}^{\infty} Q(\chi) \exp[i\chi(\xi + \alpha\tau)] \, d\chi \right\} = -M\delta(\xi)U_{\tau\tau}. \quad (4.13)$$

Here, $U(z, \tau)$ is the vertical displacement of the string, $2\mu\nu$ is the dimensionless low viscosity of the elastic foundation of the string, and $-M\delta(\xi)U_{\tau\tau}$ is the vertical force of inertia that affects the mass in the moving coordinate system.

The solution to (4.13) can be found by the mean field method according to which the string displacement should be represented as a sum of the mean field and a small fluctuation field $U = \langle U \rangle + \mu U^1$. Substituting this representation into (4.13) and performing operations described in the previous Section, we obtain the following expressions for the mean and fluctuation fields:

$$\langle U \rangle_{\tau\tau} - 2\alpha \langle U \rangle_{\tau\xi} - (1 - \alpha^2)\langle U \rangle_{\xi\xi} + 2\mu\nu(\langle U \rangle_{\tau} - \alpha \langle U \rangle_{\xi}) + \langle U \rangle + \mu^2 \left\langle U^1 \int_{-\infty}^{\infty} Q(\chi) \exp[i\chi(\xi + \alpha\tau)] \, d\chi \right\rangle = -M\delta(\xi)\langle U \rangle_{\tau\tau}, \quad (4.14)$$

$$U_{\tau\tau}^1 - 2\alpha U_{\tau\xi}^1 - (1 - \alpha^2)U_{\xi\xi}^1 + U^1 = -\langle U \rangle \int_{-\infty}^{\infty} Q^*(\chi_1) \exp[-i\chi_1(\xi + \alpha\tau)] \, d\chi - M\delta(\xi)U_{\tau\tau}^1. \quad (4.15)$$

Application of the integral Fourier transformations with respect to time and coordinate (4.14), (4.15)

$$\left\{ \langle V_{\omega}(\omega, \xi) \rangle, V_{\omega}^1(\omega, \xi) \right\} = \int_{-\infty}^{\infty} \left\{ \langle U(\xi, \tau) \rangle, U^1(\xi, \tau) \right\} \exp i\omega\tau \, d\tau,$$

$$\left\{ \langle W_{\omega, k}(\omega, k) \rangle, W_{\omega, k}^1(\omega, k) \right\} = \int_{-\infty}^{\infty} \left\{ \langle V_{\omega}(\omega, \xi) \rangle, V_{\omega}^1(\omega, \xi) \right\} \exp(-ik\xi) \, d\xi,$$

yields equations for the mean and fluctuation fields in Fourier transforms:

$$\begin{aligned} & \left[A(\omega, k) - 2i\mu\nu(\omega + \alpha k) \right. \\ & \left. + \mu^2 \int_{-\infty}^{\infty} \langle Q(\chi) W_{\omega, k}^1(\omega + \alpha k, k - \chi) \rangle d\chi \right] \langle W_{\omega, k}^0(\omega, k) \rangle \\ & = M\omega^2 \langle V_{\omega}(\omega, 0) \rangle, \end{aligned} \tag{4.16}$$

$$\begin{aligned} A(\omega, k) W_{\omega, k}^1(\omega, k) & = M\omega^2 V_{\omega}^1(\omega, 0) \\ & - \int_{-\infty}^{\infty} Q^*(\chi_1) \langle W_{\omega, k}(\omega - \alpha\chi_1, k + \chi_1) \rangle d\chi_1, \end{aligned} \tag{4.17}$$

where

$$A(\omega, k) = -\omega^2 - 2\alpha\omega k + (1 - \alpha^2)k^2 + 1.$$

Our purpose is to obtain the following equation which describes mass vibrations on the average: $\langle V_{\omega}(\omega, 0) \rangle Z(\omega) = 0$, and to use it for the estimation of the frequencies of mass oscillations [by making $Z(\omega)$ equal to zero]. The derivation procedure for this equation is described in detail in Ref. [32]. Therefore, we pass straight to the expression for $Z(\omega)$

$$\begin{aligned} Z(\omega) & = 1 - M\omega^2 \Phi \left\{ \frac{1}{A(\omega, k)} \right\} - 2i\mu\nu \Phi \left\{ \frac{\omega + \alpha k}{A(\omega, k)} \right\} \\ & - \mu^2 M \int_{-\infty}^{\infty} S(\chi) \left[\Phi \left\{ \frac{1}{A^2(\omega, k) A(\omega + \alpha\chi, k - \chi)} \right\} \right. \\ & \left. + \frac{\omega^2(\omega + \alpha\chi)^2 \Phi^2 \{ 1/[A(\omega, k + \chi) A(\omega + \alpha\chi, k)] \}}{1 - M(\omega + \alpha\chi)^2 \Phi \{ 1/A(\omega + \alpha\chi, k) \}} \right] d\chi, \end{aligned} \tag{4.18}$$

where the notation

$$\Phi[f(\omega, k)] = \frac{1}{2\pi} \int_{-\infty}^{\infty} f(\omega, k) dk$$

is used.

The roots of the equation $Z(\omega) = 0$ determine mass vibration stability. If at least one root has a positive imaginary part, mass vibrations are unstable on the average.

In the zero approximation ($\mu = 0$), the roots of the equation $Z(\omega) = 0$ are defined by the following expression (the integral $\Phi[1/A(\omega, k)]$ needs to be calculated and the resulting equation needs to be solved to find the roots):

$$\Omega = \pm \frac{\sqrt{2}}{M} \sqrt{[1 + M^2(1 - \alpha^2)]^{1/2} - 1}, \tag{4.19}$$

which, naturally, coincides with (3.24). Expression (4.19) indicates that when a mass moves along a string resting on a homogeneous elastic foundation, it undergoes vertical harmonic oscillations at $\tau \rightarrow \infty$.

Now, let us find a correction for the mass oscillation frequency introduced by small viscosity and random inhomogeneity of the foundation. For this, the roots of the equation $Z(\omega) = 0$ at $\mu \neq 0$ must be sought in the form

$$\omega = \Omega + \mu\delta. \tag{4.20}$$

We are interested in the imaginary part of δ , because it is this part that determines the stability of mass vibrations. The substitution of (4.20) into (4.18) (assuming that $\omega = \Omega$ in the terms at μ and μ^2) and calculation of integrals in (4.18) (see Ref. [32] for more details) leads to

$$\begin{aligned} \text{Im}(\delta) & = - \frac{\nu M^2 \Omega^2}{(1 - \alpha^2)(2 + M^2 \Omega^2)} - \frac{\mu M^4 (1 - \alpha^2) \Omega^2}{(2 + M\Omega^2)(2 + M^2 \Omega^2)} \\ & \times \left[S(0) \frac{1}{\alpha M^4 \Omega^4} - S\left(\frac{2\Omega}{\alpha}\right) \frac{\alpha^3}{(4 + \alpha^2 M^2 \Omega^2)^2} \right]. \end{aligned}$$

Therefore, the vibrations of a mass moving uniformly along a string resting on a randomly inhomogeneous viscoelastic foundation are, on the average, unstable provided the following condition [equivalent to $\text{Im}(\delta) > 0$] is met:

$$S\left(\frac{2\Omega}{\alpha}\right) \frac{\alpha^3}{(4 + \alpha^2 M^2 \Omega^2)^2} - S(0) \frac{1}{\alpha M^4 \Omega^4} > \frac{2\nu(2 + M\Omega^2)}{\mu M^2 (1 - \alpha^2)^3}. \tag{4.21}$$

Hence, the system may lose stability if the random function $h_1(z)$ has hidden periodicity [i.e., $S(\chi)$ has the form shown in Fig. 20] and the characteristic wave number χ_0 is close to $2\Omega/\alpha$.

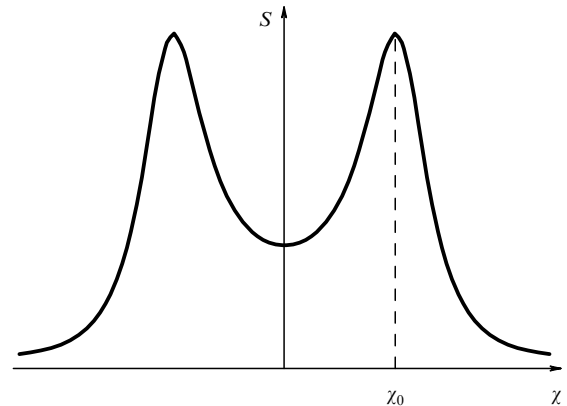


Figure 20. The correlation function spectrum for a process with hidden periodicity.

The instability zones for $S(\chi)$, which is described by the expression

$$S(\chi) = \frac{2\sigma^2}{\pi} \frac{R\chi_0^2}{(\chi^2 - \chi_0^2)^2 + 4R^2\chi^2}$$

where σ^2 is the dispersion of the process and R is the correlation radius, are illustrated in Fig. 21 for various characteristic inhomogeneity periods χ_0 ($\nu = 0$). The zones for each χ_0 are shown at $R = 0.2$ and $R = 0.25$ (they become smaller with an increase in R). It can be seen that zones of unstable mass vibrations for a string on a randomly inhomogeneous foundation are much broader than they are in the case of periodically inhomogeneous foundation (see Figs 20 and 17). However, when the elastic foundation parameters undergo random changes, the size of instability zones exhibits strong dependence on the correlation radius of the inhomogeneity. Moreover, there is a critical correlation radius $R^* = \chi_0/\sqrt{2}$ for each χ_0 beyond which there can be no instability whatever.

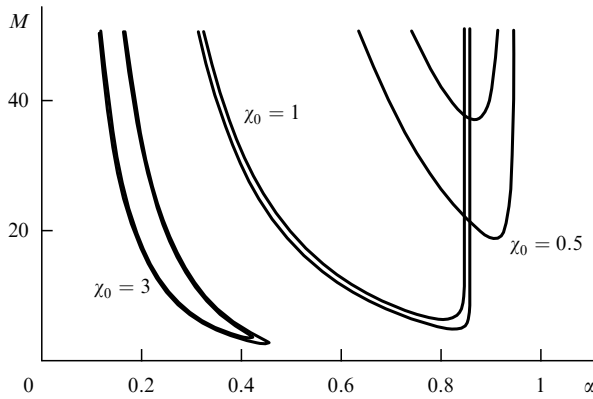


Figure 21. The main zone of mass vibration instability for different characteristic inhomogeneity periods and correlation radii.

In summary, the uniform motion of a mass along a string resting on a randomly inhomogeneous foundation whose stiffness has hidden periodicity may cause instability, on the average, of vertical vibrations of the mass. Instability occurs when the characteristic frequency of stiffness alterations in the elastic foundation beneath the moving mass, $\alpha\chi_0$, approximates the doubled frequency of the eigenvibrations of the mass moving along a string that rests on a homogeneous (unperturbed) elastic foundation. The instability zones are relatively large as compared with those of a periodically inhomogeneous string foundation, but decrease substantially and finally disappear as the inhomogeneity correlation radius increases.

To conclude, the instability condition for mass oscillations (4.21) is similar to that in a system described by the stochastic analog of the Mathieu equation:

$$\ddot{x} + 2v\dot{x} + \omega_0^2 x [1 + \mu\Psi(t)] = 0,$$

where $\Psi(t)$ is a stationary process; for such a system the ‘on-the-average instability’ condition has the form [30, 31]

$$\mu^2 [S_\Psi(2\omega_0) - S_\Psi(0)] > \frac{2v}{\pi\omega_0^2},$$

and $S_\Psi(\omega)$ is the spectrum of the correlation function. This analogy suggests that vibrations of the mass on a string may be unstable not only on the average, but also when characterized by higher-order moments [33].

5. Transition radiation in two-dimensional elastic systems

Analysis of transition radiation of elastic waves in the previous Sections was carried out with reference to one-dimensional guides. In our opinion, this is the simplest way to reveal key properties of radiation in mechanical systems, formulate problems of practical importance related to the transition radiation of elastic waves, and concurrently describe the behaviour of real structures (overhead contact wires and their supporting elements, rails, etc.). However, it should be emphasized that certain fundamental questions cannot be answered unless two-dimensional (three-dimensional) elastic systems are explored. For example, as a train moves into a tunnel in rocks, it does not necessarily traverse a boundary between the soft ground and the rock bed in the perpendicular direction. What is the angle at which radiation is emitted under these conditions? What should be the force

necessary in this case to maintain the uniform motion of the train? How does the loss of contact between the wheels and the rails depend on the angle at which the train enters the tunnel? All these questions are of practical importance and not easy to answer. Moreover, the passage of a moving object across an inhomogeneity region is not the sole source of radiation in non-one-dimensional systems; it is just as likely to arise when the object passes near this region. Such radiation is considered to be a ‘subspecies’ of transition radiation and is referred to as diffraction radiation [34]. Diffraction radiation of elastic waves occurs, for example, when a train passes settlements, stations, etc. and its deformation field affects the foundations of nearby buildings. This radiation is especially intense in the case of reciprocal diffraction of the deformation fields generated by two trains moving in opposite directions.

This section deals with two problems. First, the motion of a mass along a semibounded plate lying on an elastic foundation and fixed at its edge is considered in order to analyze the phenomenon of transition radiation in two-dimensional elastic systems. Another objective is to demonstrate conditions for the production of diffraction radiation of elastic waves and analyze its direction diagram using the model of a load moving along a spring-supported membrane fixed along a half-line.

5.1 Transition radiation in a semibounded plate. Spectral angular density of radiation energy, radiation reaction, the loss of contact between the plate and moving mass

In electrodynamics and acoustics, the radiation field far from a source is of primary interest for the analysis of transition radiation, whereas the problem of divergence at the source location associated with the jump of dimensionality (point source, three-dimensional medium) is of minor importance. The situation is different in mechanics, where information about dynamic processes in the vicinity of the source is crucial. Therefore, for an elastic system – moving object model to be of practical importance, it must provide a finite deformation field near the object. There are two ways to meet this requirement when analyzing two-dimensional systems: (1) to regard the moving object to be non-pointlike (the common approach in physics) and (2) to take into account flexural rigidity of the elastic system and describe its oscillations by fourth-order equations in spatial variables. We will use the latter approach, which is natural for mechanics because flexural rigidity is to a certain degree inherent in all elastic guides.

Let us consider uniform and rectilinear motion $\mathbf{r} = \mathbf{V}t$ ($\mathbf{V} = \{V_x, V_y\}$, $\mathbf{r} = \{x, y\}$) of a point mass m subjected to a constant vertical force P on a hinged ($x = 0$) spring-supported semibounded plate of the Kirchhoff model [35] (Fig. 22). In the linear approximation, mass and plate vibrations that cause no loss of contact are described by the following system of equations [7]:

$$\begin{aligned} \rho h U_{tt} + D \Delta_{xy}^2 U + kU &= -(P + m\ddot{U}_0)\delta(x - V_x t)\delta(y - V_y t), \\ x \leq 0, \quad t \leq 0, \quad -\infty < y < \infty, \\ U(0, y, t) = U_{xx}(0, y, t) &= 0, \quad U_0(t) = U(V_1 t, V_2 t, t), \end{aligned} \quad (5.1)$$

where $U(x, y, t)$ and $U_0(t)$ are the vertical displacements of the plate and mass, respectively; ρ , h , and D are the density, thickness, and flexural stiffness of the plate; k is the stiffness of the elastic foundation per unit area; and $\Delta_{xy}^2 = (\partial^2/\partial x^2 + \partial^2/\partial y^2)^2$ is the twice-taken two-dimensional Laplacian.

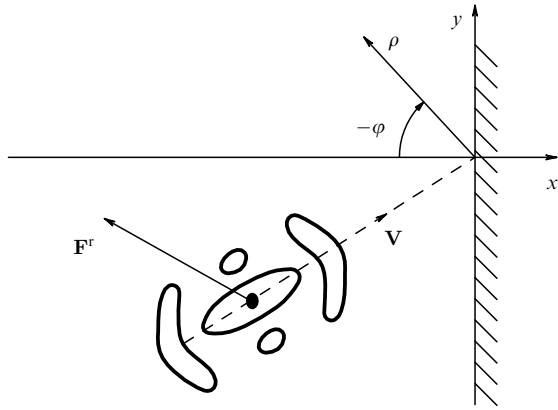


Figure 22. Uniform and rectilinear motion of a mass on a hinged plate. Top view.

Since we are primarily interested in the pure effect of transition radiation, we assume that the mass speed does not exceed the lowest phase velocity of flexural waves in the plate, i.e., $|\mathbf{V}| < \sqrt{2\mu v}$, where $\mu^2 = k/\rho h$ and $v^2 = D/\rho h$. In this range of speeds and far from the clamp, the moving mass carries its deformation eigenfield depicted qualitatively in Fig. 23 and described by the following equation [36]:

$$U^P(\xi, \eta) = \frac{m(I_1 + I_2)}{8\pi},$$

$$I_1 = -2 \int_0^{\pi/2} \cos\left(\frac{p \cos \varphi}{V}\right) \times \operatorname{Re} \left[\frac{\exp(is_1|p|/V)}{s_1} - \frac{\exp(is_2|q|/V)}{s_2} \right] d\varphi,$$

$$I_2 = \int_0^\infty \frac{\cos(p\sqrt{z^2+1})}{\sqrt{z^2+1}} \times \operatorname{Re} \left[\frac{\exp(-is_3|p|/V)}{s_3} - \frac{\exp(-is_4|q|/V)}{s_4} \right] dz,$$

$$\xi = (x - V_x t) \sqrt{\frac{\mu}{v}}, \quad \eta = (y - V_y t) \sqrt{\frac{\mu}{v}},$$

$$p = \xi \cos \theta + \eta \sin \theta, \quad q = -\xi \sin \theta + \eta \cos \theta,$$

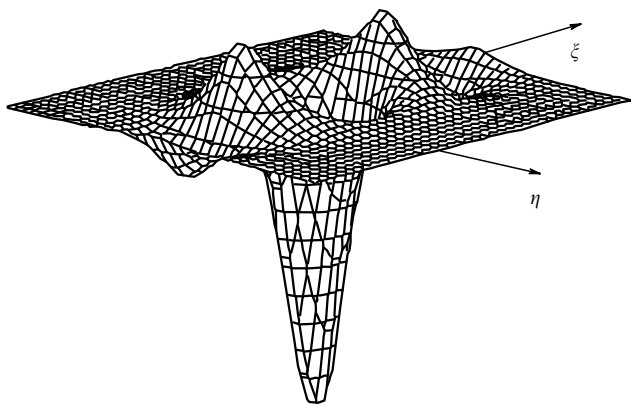


Figure 23. The deformation eigenfield of a constant load in a plate resting on an elastic foundation.

$$\tan \theta = \frac{V_y}{V_x}, \quad V = |\mathbf{V}|, \quad s_{1,2} = \sqrt{-\cos^2 \varphi \mp 2iV^2 \sin \varphi},$$

$$\operatorname{Im}(s_{1,2}) > 0, \quad s_{3,4} = \sqrt{z^2 \mp 2V^2 z + 1}. \quad (5.2)$$

The angle θ (the angle of incidence) is measured counterclockwise.

In analogy to the analysis of transition radiation in a string (Section 2.1), we suppose that $|m\ddot{U}_0| \ll P$, i.e., the effect of mass inertia is small. In the framework of this assumption, the horizontal reaction of the plate for a moving object must be found together with the angular spectral density of radiation energy.

In order to determine the reaction of the plate, we must find its displacement $U^-(x, y, t)$ at $t < 0$. This can easily be done using the method of images, in which U^- is described by the expression

$$U^-(x, y, t) = U^P(x, y, t) - U^P(-x, y, t). \quad (5.3)$$

The substitution of (5.3) into the general expression for the horizontal reaction of the plate

$$\mathbf{F}^r = -\nabla_{xy} U(x, y, t)_{x=V_x t, y=V_y t},$$

leads to

$$\mathbf{F}^r = \{F_x, F_y\} = -\nabla_{xy} U^-(x, y, t)_{x=V_x t, y=V_y t} = \nabla_{xy} U^P(-x, y, t)_{x=V_x t, y=V_y t}. \quad (5.4)$$

[$U^P(x, y, t)$ is symmetrical about the moving load and does not contribute to the horizontal reaction of the plate]. The qualitative picture of the force \mathbf{F}^r calculated from (5.4) is shown in Fig. 24 for the case of the ‘oblique fall’ of the load onto the clamp. The function $\mathbf{F}^r(t)$ (t is a parameter) is defined parametrically. It can be seen that the horizontal reaction of the plate alters in the course of the load’s motion in terms of both the magnitude and the direction, which is not typical of the electrodynamics and acoustics.

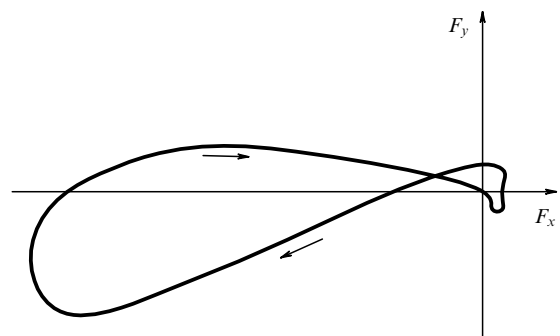


Figure 24. The plate’s horizontal reaction for a moving load.

Thus, the uniform rectilinear motion of an object near a clamp is maintained by the external force R variable in strength and direction. Results of the analysis indicate that this force must grow as the object approaches the fixed support, whereas the rate of this change (both in magnitude and direction) increases with decreasing the incidence angle θ .

The angular spectral density of radiation energy $S_{\omega, \varphi}$ can be calculated by the method given in Ref. [1]. A detailed procedure is described in Ref. [36]. Here, we only cite the final

expression for $S_{\omega, \varphi}$ (φ is the angle between the radiation wave vector and the normal to the line of clamp, which is measured counterclockwise):

$$S_{\omega, \varphi}(\omega, \varphi) = \frac{F^2 \alpha^2}{4\pi^2 \cos^2 \theta} \omega \cos^2 \varphi \times \left\{ \frac{[\omega + \alpha \sin \theta \sin \varphi (2\omega^2 - 1)^{1/4}]^2}{\cos^2 \theta} - \alpha^2 \cos^2 \varphi \sqrt{2\omega^2 - 1} \right\}^{-2}.$$

This expression contains parameters $F = P^2/(\sqrt{2} \rho h \mu^2 v)$, $\omega = \tilde{\omega}/\mu\sqrt{2}$ ($\tilde{\omega}$ is the frequency), and $\alpha = V/\sqrt{2\mu v}$ is the dimensionless load speed. In order to obtain the total radiation energy W^r , its angular spectral density $S_{\omega, \varphi}$ must be integrated in the following way:

$$W^r = \int_{1/\sqrt{2}}^{\infty} \int_{-\pi/2}^{\pi/2} S_{\omega, \varphi}(\omega, \varphi) d\omega d\varphi.$$

The variation of the angular spectral density of radiation energy as a function of the angle φ ($\omega = \text{const}$) is depicted in Fig. 25 for the ‘incidence angle’ of the load onto the line of clamp $\tau = \pi/4$. The three curves correspond to three different load speeds. The radiation energy grows as the angle approaches $\varphi = -\theta$, and the ‘angle of incidence is equal to the angle of reflection’ rule is satisfied the better the closer the load speed is to the critical value. Thus, at subcritical speeds coupled to high radiation power, the energy is mainly emitted in the direction which mirrors (with respect to the normal to the line of clamp) the direction of the load. At low speeds, the angular distribution of radiation energy is virtually uniform.

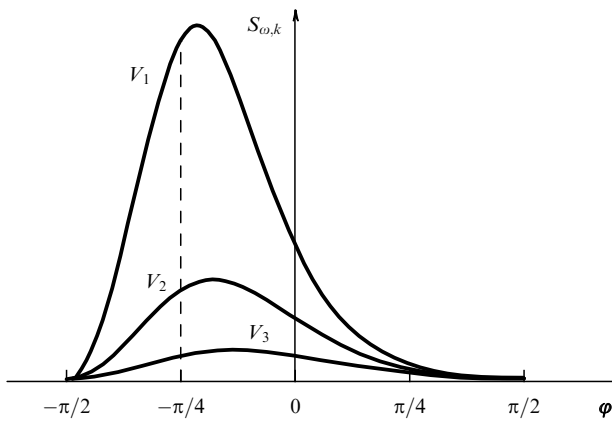


Figure 25. Angular spectral density of radiation energy at a constant frequency for different velocities of motion: $V_1 > V_2 > V_3$, $\theta = \pi/4$.

If the problem (5.1) is examined in its original formulation (taking into account mass inertia), the vertical mass oscillations are described by the following integro-differential equation (its derivation as described in Ref. [36] is similar to that used in Section 2.3):

$$U_0(T) = U^-(\alpha_x T, \alpha_y T, T) + 2M \int_{-\infty}^T \ddot{U}_0(\tau) \left\{ G[\alpha_x(T+\tau), \alpha_y(T-\tau), T-\tau] - G[\alpha_x(T-\tau), \alpha_y(T-\tau), T-\tau] \right\} d\tau,$$

$$G(\mathbf{r}, T) = \frac{1}{2\sqrt{2}\pi} \int_0^{\infty} \frac{z J_0(z|\mathbf{r}|)}{\sqrt{z^4 + 1}} \sin\left(\frac{T\sqrt{z^4 + 1}}{\sqrt{2}}\right) dz, \quad (5.5)$$

where $T = t\mu/\sqrt{2}$ is dimensionless time, $\alpha_{x,y} = V_{x,y}/\sqrt{2\mu v}$ are the dimensionless projections of load speed, $M = m\mu/vph$ is the dimensionless mass, τ is the dimensionless integration variable, U^- is defined by expression (5.3), and G is the zero-order Bessel function.

Eqn (5.5) may be used to find the dependence $\ddot{U}_0(t)$ and determine [from the condition $P + m\ddot{U}_0 = 0$, see (4.1)] the parameters of the problem responsible for the loss of contact between the mass and the plate at $t < 0$. Figure 26 shows the curves $M = M^*(\alpha)$ dividing the plane of parameters (M, α) into the regions of contact (under the curve) and noncontact (above the curve) motion at different angles of load ‘incidence’ θ . Evidently, the region of contact motion broadens with increasing angle of incidence θ . Therefore, the oblique passage of an object across the line of clamp (in the general case, an inhomogeneity region) entails a lower risk of loss of contact than crossing in the perpendicular direction.

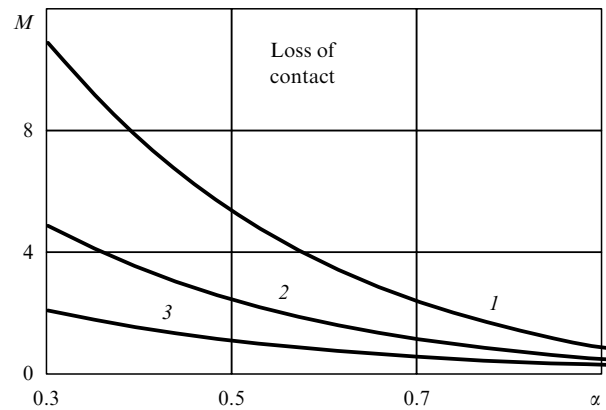


Figure 26. Curves dividing the plane of parameters into regions of contact and non-contact motion at different ‘incidence angles’: (1) $\theta = \pi/3$; (2) $\theta = \pi/6$; and (3) $\theta = \pi/18$.

In summary, analysis of transition radiation in a two-dimensional elastic system has demonstrated that (a) a moving load is subjected to the horizontal reaction of the elastic system which is variable in both the magnitude and direction, (b) the maximum radiation energy at subcritical load speeds is achieved at an angle which is mirrored in the ‘angle of incidence’, (c) the speed at which the object loses contact with the elastic system decreases (other things being equal) as the ‘incidence angle’ increases.

5.2 Motion of constant load over a membrane clamped along a half-line (diffraction radiation). Direction diagram of radiation

An analysis of transition radiation has demonstrated that it results from the transformation of the deformation eigenfield of a moving perturbation source. It is this field, rather than the source itself, that is responsible for the generation of transition radiation. It arises even when the field undergoes restructuring caused by inhomogeneities (in mechanics: supports, stiffeners, etc.) near the source’s path even though the medium properties directly on the trajectory remain unaltered. This radiation is called diffraction radiation.

Studies of diffraction radiation of elastic waves have but a short history [37]. Therefore, this review is confined to an analysis of the simplest model which allows one to demonstrate the radiation effect and analyze its direction diagram.

Let us consider a membrane resting on an elastic foundation with stiffness k and fixed along a ray [half-line ($\xi_+ = \{x > 0, y = 0\}$)]. Let us further assume that a constant vertical load P moves rectilinearly and uniformly across the membrane at speed $\mathbf{V} = \{V_x, V_y\}$ (Fig. 27). In this case, forced membrane vibrations are described by the following system of equations:

$$\Delta_{x,y} U - \frac{1}{c^2} U_{tt} - \mu^2 U = F \delta(\mathbf{r} - \mathbf{a} - \mathbf{V}t),$$

$$-\infty < x, y, t < \infty,$$

$$U(x, y, t)|_{\xi_+} = 0, \quad c^2 = \frac{N}{\rho}, \quad \mu^2 = \frac{k}{N}, \quad (5.6)$$

where $U(x, y, t)$ is the displacement of the membrane; $\Delta_{x,y}$ is the two-dimensional Laplacian; ρ and N are the membrane surface density and tension, respectively; $F = P/N$; $\mathbf{a} = \{a_x, a_y\}$ is the distance from the origin to the load path; $\mathbf{r} = \{x, y\}$ is the radius vector; and the motion is assumed to be subcritical, i.e., $V = |\mathbf{V}| < c$.

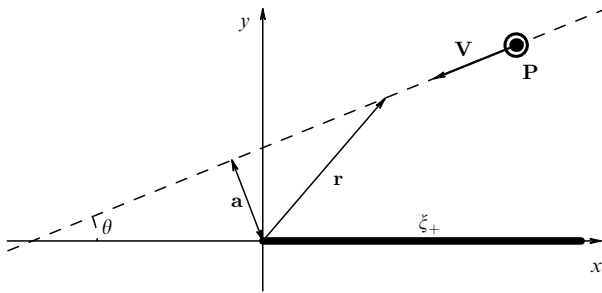


Figure 27. The motion of a load across a spring-supported membrane clamped along a half-line. Top view.

The solution to (5.6) is sought as the sum of the eigenfield of the load U^P and the field U^r generated due to the interaction between the eigenfield and the clamp:

$$U = U^P + U^r. \quad (5.7)$$

The eigenfield U^P is a steady-state field of displacements that moves with the load over a boundless unclamped part of the membrane lying on an elastic foundation. According to [37], it is described by the expression

$$U^P(\mathbf{r}, t) = -\frac{F}{4\pi V} \int_{-\infty}^{\infty} \frac{1}{\lambda(\omega)} \times \exp \left[i\omega \left(\frac{(\mathbf{V}, \mathbf{r})}{V^2} - \lambda(\omega) \left| \frac{(\mathbf{a}, \mathbf{r})}{a} - a \right| \right) \right] \exp(-i\omega t) d\omega,$$

$$\lambda(\omega) = \sqrt{\mu^2 + \frac{\omega^2(1 - \alpha^2)}{V^2}}, \quad a = |\mathbf{a}|, \quad \alpha = \frac{V}{c}. \quad (5.8)$$

By substituting (5.7) into (5.6) and using the Fourier transformation with respect to time and coordinate x , we obtain a system of equations for the Fourier transform of the

field U^r

$$\frac{\partial^2}{\partial y^2} W_{\omega,k}^r - \left(k^2 + \mu^2 - \frac{\omega^2}{c^2} \right) W_{\omega,k}^r = 0,$$

$$W_{\omega,k}^r(\omega, k, y)|_{\xi_+} = -W_{\omega,k}^P(\omega, k, y)|_{\xi_+}, \quad (5.9)$$

where

$$W_{\omega,k}^{P,r}(\omega, k, y) = \int_{-\infty}^{\infty} \int_{-\infty}^{\infty} U^{P,r}(x, y, t) \exp(i\omega t - ikx) dx dt.$$

Bearing in mind the constraint on the membrane displacement at infinity (for the vibrations localized near the clamp) and energy removal from the clamp (for waves), the solution of (5.9) can be written in the form

$$W_{\omega,k}^r = A(\omega, k) \exp(-\gamma|y|), \quad \gamma = (k - b)^{1/2}(k + b)^{1/2},$$

$$b = \left(\frac{\omega^2}{c^2} - \mu^2 \right), \quad \text{Re}(\gamma) > 0 \quad \forall k.$$

The unknown function $A(\omega, k)$ is found by the Wiener-Hopf method [38], which leads to the system of integral equations with respect to $A(\omega, k)$

$$\frac{1}{2\pi} \int_{-\infty}^{\infty} A(\omega, k) \exp ikx dk = \frac{F}{2V\lambda(\omega)} \exp \left[-i \frac{\omega x}{V} \cos \theta - \lambda(\omega)(x \sin \theta + a) \right],$$

$$x > 0, \quad y = 0, \quad (5.10)$$

$$\frac{1}{2\pi} \int_{-\infty}^{\infty} A(\omega, k) \gamma(\omega, k) \exp ikx dk = 0, \quad x < 0, \quad y = 0, \quad (5.11)$$

where θ is the angle between the load path and the axis x (see Fig. 27). Eqn (5.10) is obtained by the inverse Fourier transformation with respect to the coordinate x of the boundary condition (5.10), whereas Eqn (5.11) reflects the continuity of the normal derivative of the plate displacement at $\{x < 0, y = 0\}$ (the membrane is not fixed at this straight half-line).

It follows from (5.11) that the function $A(\omega, k)\gamma(\omega, k)$ has no poles in the lower half-plane of the complex variable k ; therefore, $A(\omega, k)$ must have the form

$$A(\omega, k) = \frac{C(\omega)L(\omega, k)}{\gamma(\omega, k)}, \quad (5.12)$$

where $L(\omega, k)$ has no poles in the lower half-plane of k . The selection of the form of the function $L(\omega, k)$ in such a way as to satisfy Eqn (5.10) leads to

$$L(\omega, k) = \frac{(k - b)^{1/2}}{k - k_0}, \quad k_0 = i\lambda(\omega) \sin \theta - \frac{\omega}{V} \cos \theta. \quad (5.13)$$

Determining $C(\omega)$ by substituting (5.12), and (5.13) into (5.10), we obtain the following final expression for $A(\omega, k)$:

$$A(\omega, k) = -\frac{iF \sqrt{k_0 c + (\omega^2 - h^2)^{1/2}} \exp[-a\lambda(\omega)]}{2V\lambda(\omega)(k - k_0) \sqrt{kc + (\omega^2 - h^2)^{1/2}}},$$

$$h^2 = \mu^2 c^2.$$

Therefore, the Fourier transform of the membrane displacement field caused by the interaction between the eigenfield of the load and the clamp has the form

$$W_{\omega,k}^r = -\frac{iF\sqrt{k_0c + (\omega^2 - h^2)^{1/2}} \exp[-a\lambda(\omega)]}{2V\lambda(\omega)(k - k_0)\sqrt{kc + (\omega^2 - h^2)^{1/2}}} \exp(-\gamma|y|).$$

In the wave zone, this field describes diffraction radiation of elastic waves.

The radiation energy can most easily be estimated by the method described in Refs [1, 14, 37] according to which the problem reduces to a search for the emitted train of waves at large times, after it has moved away from the clamp and is unable to interfere with the eigenfield.

According to [37], the angular spectral density of radiation energy thus obtained is described by the expression

$$\begin{aligned} S_{\omega,\varphi}(\omega, \varphi) &= B\omega\sqrt{\omega^2 - h^2}(\omega - \alpha\sqrt{\omega^2 - h^2} \cos \theta) \\ &\times \sin^2 \frac{\varphi}{2} \exp[-2a\lambda(\omega)] \left[\left(h^2 + \frac{\omega^2(1 - \alpha^2)}{\alpha^2} \right) \right. \\ &\times \left\{ (\omega \cos \theta + \alpha\sqrt{\omega^2 - h^2} \cos \varphi)^2 \right. \\ &\left. \left. + [\omega^2 - \alpha^2(\omega^2 - h^2)] \sin^2 \theta \right\}^{-1} \right], \end{aligned} \quad (5.14)$$

where $B = \rho F^2 c^2 / \alpha$, φ is the angle between the radiation wave vector and the positive direction of the x axis.

An analysis of Eqn (5.14) shows that radiation has a dipole nature (Fig. 28a) at load speeds satisfying the inequality

$$\alpha = \frac{V}{c} < \alpha_{\text{cr}} = \frac{\omega(2 + \cos \theta)}{\sqrt{\omega^2 - h^2}(3 + \sin^2 \theta)},$$

whereas at $\alpha > \alpha_{\text{cr}}$ the direction diagram displays two maxima (Fig. 28b) at angles

$$\varphi = \pm \arccos \left(1 - \frac{\omega + \alpha\sqrt{\omega^2 - h^2}}{\alpha\sqrt{\omega^2 - h^2}} \cos \theta \right).$$

At $\alpha \rightarrow 1$, $\omega \rightarrow \infty$, the maxima are shifted to angles $\varphi = \pm(\pi - \theta)$, i.e., the energy is mainly emitted in the same direction in which the load moves and which mirrors the direction to the fixed half-line. The intensity of radiation falls off exponentially with increasing distance between the load path and the fixed half-line support.

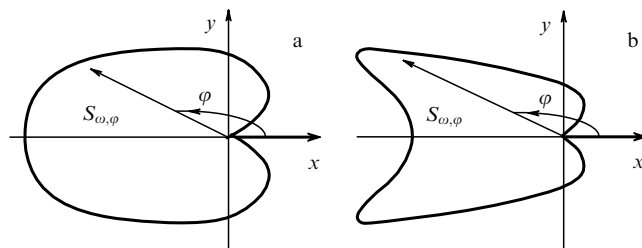


Figure 28. Radiation direction diagrams at different load speeds: (a) $\alpha < \alpha_{\text{cr}}$, (b) $\alpha > \alpha_{\text{cr}}$.

6. Conclusion

Two kinds of reactions were encountered when the foregoing material was presented at various workshops. Physicists focused attention on important practical implications of the effect, while showing no apparent interest in its specific manifestations in mechanical systems and problems requiring further study. On the contrary, mechanics showed the ability to appreciate the beauty of the analogy and perceive the ‘general physical’ nature of the effect, but wished the reported results to be interpreted not only in terms of the wave theory, but also in the context of classical mechanics. Some bluntly advised putting an end to such alien terminology in mechanics. Anticipating a similar reaction on the part of the readers, we have tried to emphasize the following aspects: (1) radiation-related resonance, unstable oscillations of perturbation sources, and the loss of contact between a moving source and a medium (elastic guide) are the most topical problems (non-classical for electrodynamics and acoustics) in the context of innovation in high-speed transportation as a sphere of application of the theory of transition radiation of elastic waves, (2) the variety of dispersion properties intrinsic in real elastic systems is responsible for the ‘non-classical’ behaviour of classical radiation parameters (as exemplified by the effect of radiation reaction for a load moving along a plate), and (3) the language of the wave theory is adequate to the processes whose characteristic velocity is comparable with wave velocity and makes it possible to easily clarify the physical mechanisms of such phenomena, ‘natural’ for mechanics, as resonance and unstable vibrations of an object moving in an elastic system.

The scope of important practical problems related to transition radiation of elastic waves is actually much broader than that discussed in this review. The question at issue now turns on supercritical velocities (velocities of surface waves) of high-speed trains. Preliminary studies indicate that the transition through the critical speed is easier to accomplish by modulating railroad track parameters, without subjecting passengers to acceleration overloads. Of special interest in this context is the problem of transition radiation (and its interference with Cherenkov radiation) generated when a load crosses the inhomogeneity region and moves further at a supercritical speed, i.e., a speed exceeding wave velocity. Supercritical motion is fraught with the risk of instability due to the emission of anomalous Doppler waves [15–17] and with the resonance effect of waves reflected from inhomogeneity regions (see Ref. [39] and references therein). Studies of transition radiation in non-linear elastic systems are also of great interest, because the ballast bed of railroads is normally maintained in an elastic-plastic regime, and its conditions can be estimated from radiation parameters. Qualitative evaluation of this problem has until now been restricted to the analysis of the load’s eigenfield [40]. Finally, transition radiation analysis is needed for three-dimensional systems such as ‘a beam on an elastic half-space’ [41–43]. Such models currently provide the most complete description of railroad track dynamics.

Acknowledgements. We wish to thank the personnel of the Department of Wave Dynamics of Machines, Nizhni Novgorod Branch, Institute of Mechanical Engineering, Russian Academy of Sciences, and the Mechanics and Structures Group, Delft University of Technology, the Netherlands, for their valuable comments.

References

1. Ginzburg V L, Tsytoich V N *Perekhodnoe Izluchenie i Perekhodnoe Rasseyaniye* (Transition Radiation and Transition Scattering) (Moscow: Nauka, 1984) (Bristol, New York: A Hilger, 1990)
2. Ginzburg V L, Frank I M *Zh. Eksp. Teor. Fiz.* **16** 15 (1946)
3. Dokuchaev V P *Zh. Eksp. Teor. Fiz.* **43** 595 (1962)
4. Ginzburg V L, Tsytoich V N *Usp. Fiz. Nauk* **126** 553 (1978) [*Phys. Rep.* **49** 1 (1979)]
5. Pavlov V I, Sukhorukov A P *Usp. Fiz. Nauk* **147** 83 (1985) [*Sov. Phys. Usp.* **28** 784 (1985)]
6. Vesnitskiĭ A I, Kaplan L E, Utkin G A *Prikl. Mat. Mekh.* **47** (5) 863 (1983) [*Appl. Math. Mech.* **47** 692 (1983)]
7. Kokhmanyuk S S, Yanyutin E G, Romanenko L G *Kolebaniya Deformiruemyykh Sistem pri Impul'snykh i Podvizhnykh Nagruzkakh* (Oscillations of Deformed Systems Subjected to Pulsed and Moving Loads) (Kiev: Naukova Dumka, 1980)
8. Vesnitskiĭ A I, Metrikin A V *Zh. Prikl. Mekh. Tekh. Fiz.* (2) 62 (1992)
9. Denisov G G *Izv. Akad. Nauk SSSR Mekh. Tverd. Tela* **29** (1) 42 (1994) [*Mech. Solids* **29** 36 (1994)]
10. Biderman V L *Teoriya Mekhanicheskikh Kolebanii* (The Theory of Mechanical Oscillations) (Moscow: Vysshaya Shkola, 1980)
11. *Vibratsii v Tekhnike. Spravochnik* Vol. 1 (Vibrations in Technique. Reference Book) (Moscow: Mashinostroenie, 1978)
12. Bogacz R, Krzyzyski T, Popp K, in *Proc. of the 2nd German–Polish Workshop at Paderborn* (March, 1991) p. 105
13. Knothe K I, Grassie S *Vehicle System Dynamics* **22** 209 (1993)
14. Ginzburg V L *Teoreticheskaya Fizika i Astrofizika* (Theoretical Physics and Astrophysics) (Moscow: Nauka, 1981)
15. Denisov G G, Kugusheva, Novikov V V E K *Prikl. Mat. Mekh.* **49** (4) 691 (1985) [*Appl. Math. Mech.* **49** 533 (1985)]
16. Bogacz R, Nowakowski S, Popp K *Acta Mech.* **61** 117 (1986)
17. Metrikin A V *Akust. Zh.* **40** (1) 99 (1994) [*Acoust. Phys.* **40** (1) 85 (1994)]
18. Jezequel L *Trans. ASME J. Appl. Mech.* **48** 613 (1981)
19. Cai C, Cheung Y, Chan H J. *of Sound and Vibration* **123** 461 (1988)
20. Vesnitskiĭ A I, Metrikin A V *Izv. Akad. Nauk SSSR Mekh. Tverd. Tela* (6) 164 (1993)
21. Metrikin A V *Zh. Prikl. Mekh. Tekh. Fiz.* (4) 176 1995
22. Vesnitskiĭ A I, Metrikin A V *Zh. Prikl. Mekh. Tekh. Fiz.* (2) 127 1993
23. Metrikin A V *Sb. st.* (Nizhniĭ Novgorod: Nf IMASH RAN, 1994) p. 19
24. Landau L D, Lifshitz E M *Mekhanika* (Mechanics) (Moscow: Nauka, 1988) (Oxford: Pergamon Press, 1976)
25. Rabinovich M I, Trubetskoy V I *Vvedenie v Teoriyu Kolebanii i Voln* (Introduction to the Theory of Oscillations and Waves) (Moscow: Nauka, 1988)
26. Vesnitskiĭ A I, Metrikin A V *Prikl. Mekh.* **28** (2) 46 1992
27. Bass F G *Izv. Vyssh. Uchebn. Zaved. Radiofiz.* **2** 656 (1959)
28. Tamoikin V V *Izv. Vyssh. Uchebn. Zaved. Radiofiz.* **6** (2) 257 (1963)
29. Vladimirov V S *Uravneniya Matematicheskoi Fiziki* (Equations of Mathematical Physics) (Moscow: Nauka, 1988)
30. Alekseev V M, Valeev K G *Izv. Vyssh. Uchebn. Zaved. Radiofiz.* **14** 1810 (1971)
31. Bolotin V V *Sluchainye Kolebaniya Uprugikh Sistem* (Random Vibrations of Elastic Systems) (Moscow: Nauka, 1979) [Translated into English (Boston: Kluwer Acad. Publ., 1984)]
32. Vesnitskiĭ A I, Metrikin A V *Izv. Akad. Nauk SSSR Mekh. Tverd. Tela* (4) (1966)
33. Klyatskin V I *Stokhasticheskie Uravneniya i Volny v Sluchaĭno-neodnorodnykh Sredakh* (Stochastic Equations and Waves in Random Inhomogeneous Media) (Moscow: Nauka, 1980)
34. Bolotovskii B M, Voskresenskiĭ G V *Usp. Fiz. Nauk* **88** 209 (1966) [*Sov. Phys. Usp.* **9** 73 (1966)]
35. Rabotnov Yu N *Mekhanika Deformiruemogo Tverdogo Tela* (Mechanics of Deformed Solid Body) (Moscow: Nauka, 1988)
36. Vesnitskiĭ A I, Kononov A V, Metrikin A V *Zh. Prikl. Mekh. Tekh. Fiz.* (3) 170 (1955)
37. Kononov A V, Metrikin A V *Izv. Russian Akad. Nauk Mekh. Tverd. Tela* (1) 52 (1996)
38. Noble B *Methods Based on the Wiener–Hopf Technique for the Solution of Partial Differential Equations* (Oxford: Pergamon Press, 1958) [Translated into Russian (Moscow: Inostr. Lit., 1962)]
39. Metrikin A V *Akust. Zh.* **40** (6) 974 (1994) [*Acoust. Phys.* **40** (6) 864 (1994)]
40. Metrikin A V *Akust. Zh.* **40** (4) 647 (1994) [*Acoust. Phys.* **40** (4) 573 (1994)]
41. Filippov A P *Izv. Akad. Nauk SSSR Mekhanika i Mashinostroenie* (6) 97 (1961)
42. Labra J J *Acta Mech.* **22** 113 (1975)
43. Dieterman H, Metrikine A *European J. Mechanics A* **15** 67 (1996)